[redacted]

ELECTRONIC MATERIALS RESEARCH LABORATORY

THE UNIVERSITY OF TEXAS

COLLEGE OF ENGINEERING

AUSTIN

RESEARCH ON DIGITAL TRANSDUCER PRINCIPLES

VOLUME II

FIRST ANNUAL REPORT

for the

NATIONAL AERONAUTICS AND SPACE ADMINISTRATION

GRANT NGR-44-012-043

Covering the Period

January 1, 1967 - June 30, 1967

by

William H. Hartwig

Project Director

The University of Texas

Austin, Texas 78712

TABLE OF CONTENTS

ABSTRACT

The first year of work under Grant NGR-44-012-043 was completed with the development of several workable digital device concepts and considerable experimental and theoretical evidence that thin-film structures held real hope for useful digital device applications. The First Semiannual Report, Volume I of this set, contains the basis for these ideas and Volumes III and IV are detailed accounts of charge transport processes in thin films of a polymer and of Silicon Nitride. This report, Volume II covers the growth of ideas and results of related work carried out during the last six months of the year.

The efforts have been directed along three lines; continued work on thin-film transport in polymer dielectrics, fabrication of semiconductor devices which have digital or discontinous response along with mathematical models to account for their behavior, and development of capability to deposit exotic dielectrics films by chemical vapor deposition.

Chemical vapor deposition of new materials has been successfully accomplished during the second six month of the project. The period was largely spent in setting up experimental facilities, and these have had some initial use which resulted in thin films of titanium dioxide.

An entirely new digital transducer concept has been added to those already being studied. Work previously in progress in the laboratory on optical effects in semiconductors has revealed a photodielectric effect which can be used to convert analog light intensity into frequency changes or phase changes, depending upon the material. The transducer, therefore, would accept either analog light

intensity or integrated light energy for a short period and produce a frequency change which would be read out as a number of axis crossings in a selected interval. For example, if a light changed intensity by an arbitrary amount, a digital measurement would be made as frequency proportional to the integrated light intensity in the flash, regardless of its duration. The previous application of a similar phenomenon, photoconductivity, would produce only an analog change in output voltage level proportional to the input light changes. The ability of a semiconductor to display a photoreactive circuit behavior, means that a frequency change instead of a power or voltage level change results. The frequency change is inherently a digital response which is read out as a number of events per unit. An unexpected property of one of the photodielectric materials (CdS with Ag impurities) is its discontinous response to mechancial shock. The frequency change after a period of illumination could be reset by a sharp blow. The digital transducer applications of this are very interesting and require further intensive study.

The results after one year of research can be summarized as being very promising. Digital behavior of materials has appeared in a wide variety of forms and in many cases the applications to transducer concepts follows after only a modest effort. The digital temperature and magnetic field transducers, which operate in a cryogenic environment, are examples which are described in Vol. I. Others have promising futures, but their novelty is accompanied by a void in documented theory and measurement. Considerable work lies ahead to explain the basic solid state physics of the phenomena and reduce the new scientific knowledge to practice.

I. POLYMER FILM RESEARCH

Essential to thin film digital devices is an understanding of charge transport processes through the dielectric film. The silicone polymer described in Volumes I and III has been the subject of continued study for several reasons; it is a very convenient material to deposit in thin film form on any substrate, it has fundamental charge transport problems which may enrich the knowledge of dielectric materials, and the technique may generate a wide variety of yet undiscovered polymers. It has already been shown useful in the metal-polymer-semiconductor digital device. The material is relatively unstudied, however, and some effort has been made to relate the mechanism of polymerization to the structure and dielectric properties. Extensive work has been done which necessitated the separate Volume III for the report on this phase.

The polymer films have been grown on both silicon and evaporated metal-on-glass substrates. The latter metal-polymer-metal configurations have been measured as a function of frequency, thickness, and aging to evaluate the transport mechanism present, separation of bulk and surface effects, and to consider how these will be useful in device design. There are several mechanisms which are important in charge transport through dielectric films, which are discussed in Volumes III and IV. It is apparent we can make dielectric films which have all of these mechansisms present. This has the decided advantage of giving the device designer some choice of mathematical function which would suit the application, since these mechanisms have different dependences on thickness, voltage, temperature and structure, whether bulk or surface. In all cases it is possible to have a very steeply increasing current as a function of voltage. This can be followed, at some critical voltage, by a separate behavior, as discussed in Volume I, which is more nearly a constant-current relation. This is

the basis for digital action. The results of measurements show a consistent aging effect which appears to be associated with surface changes, probably adsorption of gases or water vapor. The change in capacitance with time is only a few percent of the total capacity, but the absolute change is essentially independent of thickness. The Dissipation Factor, on the other hand, seems to be more nearly a bulk effect. The frequency dependence of the dielectric constant and the Dissipation Factor are being examined for clues to the relation between them and the structure of the polymer. There is little known about this class of plastic growth process, in which liquid molecules are polymerized in a vacuum by a beam of electrons. As a result the entire effort can add to knowledge of polymers and their structure. Another possibility is that not enough can be learned to answer all the questions which must be answered to permit this very convenient technology to be exploited. The polymer itself is very durable and can be grown at precise rates with little tendency to form pinholes. It is felt this phase of the project would yield some unexpected returns if it became possible to grow thin film dielectrics with predictable properties which could then be used routinely. So far the most significant finding is a consistent change in the slope of capacity vs frequency near 2000Hz. This is apparently a characteristic response and is being studied for cause-and-effect relations. So far the scatter in the Dissipation Factor vs frequency data has made it difficult to determine the functional relation.

During the second six months of the year more mechanisms were developed to produce a discontinuity in the I-V characteristic. It was shown in Volume I that a depletion layer forming in a reverse-biased MPS device would cause the current to saturate. We have now seen that the series resistance of the semiconductor in the forward bias condition produces a similar response. This occurs

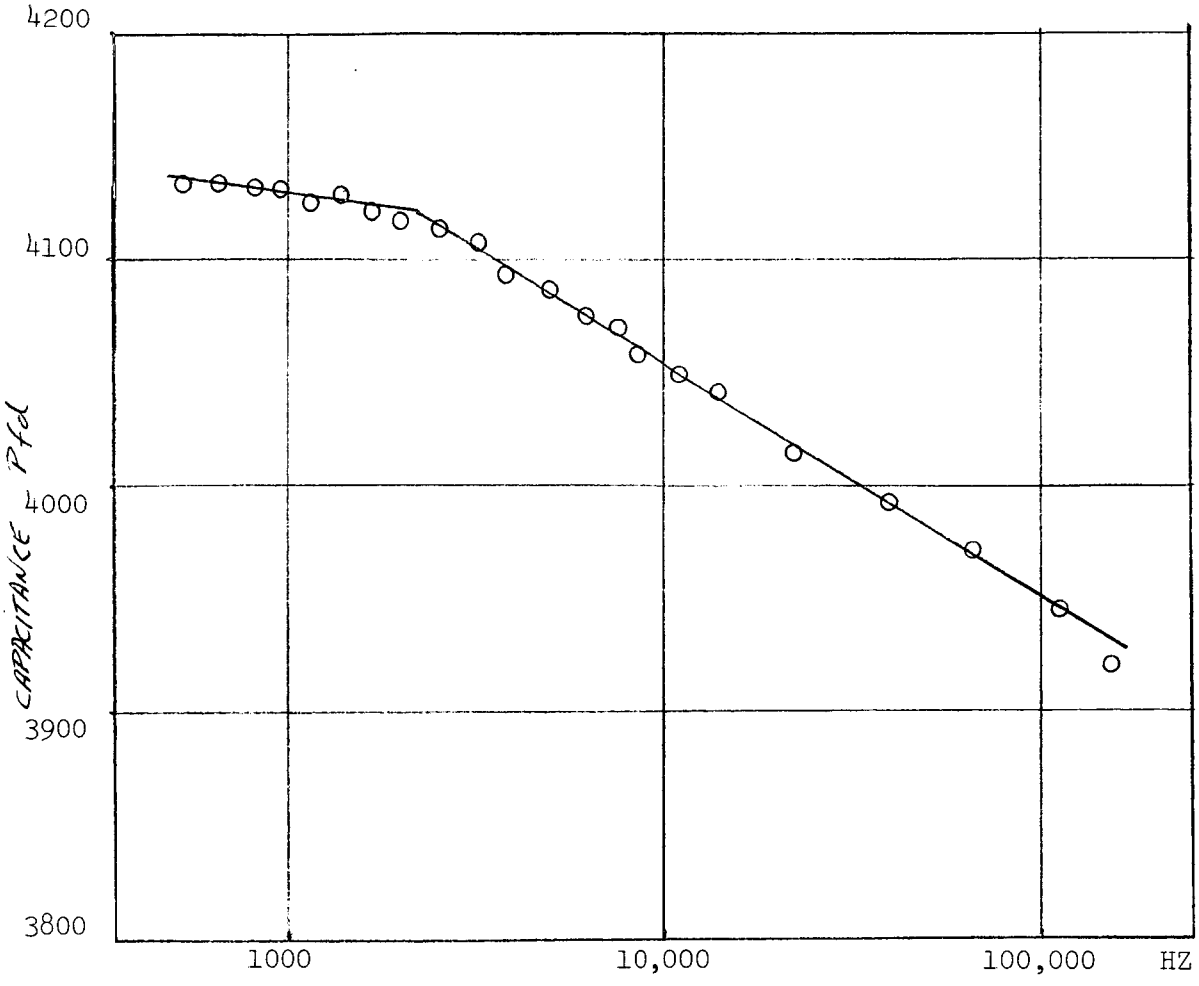

Figure 1 C vs Frequency for a Typical Sample Capacitor with Silicone Polymer dielectric

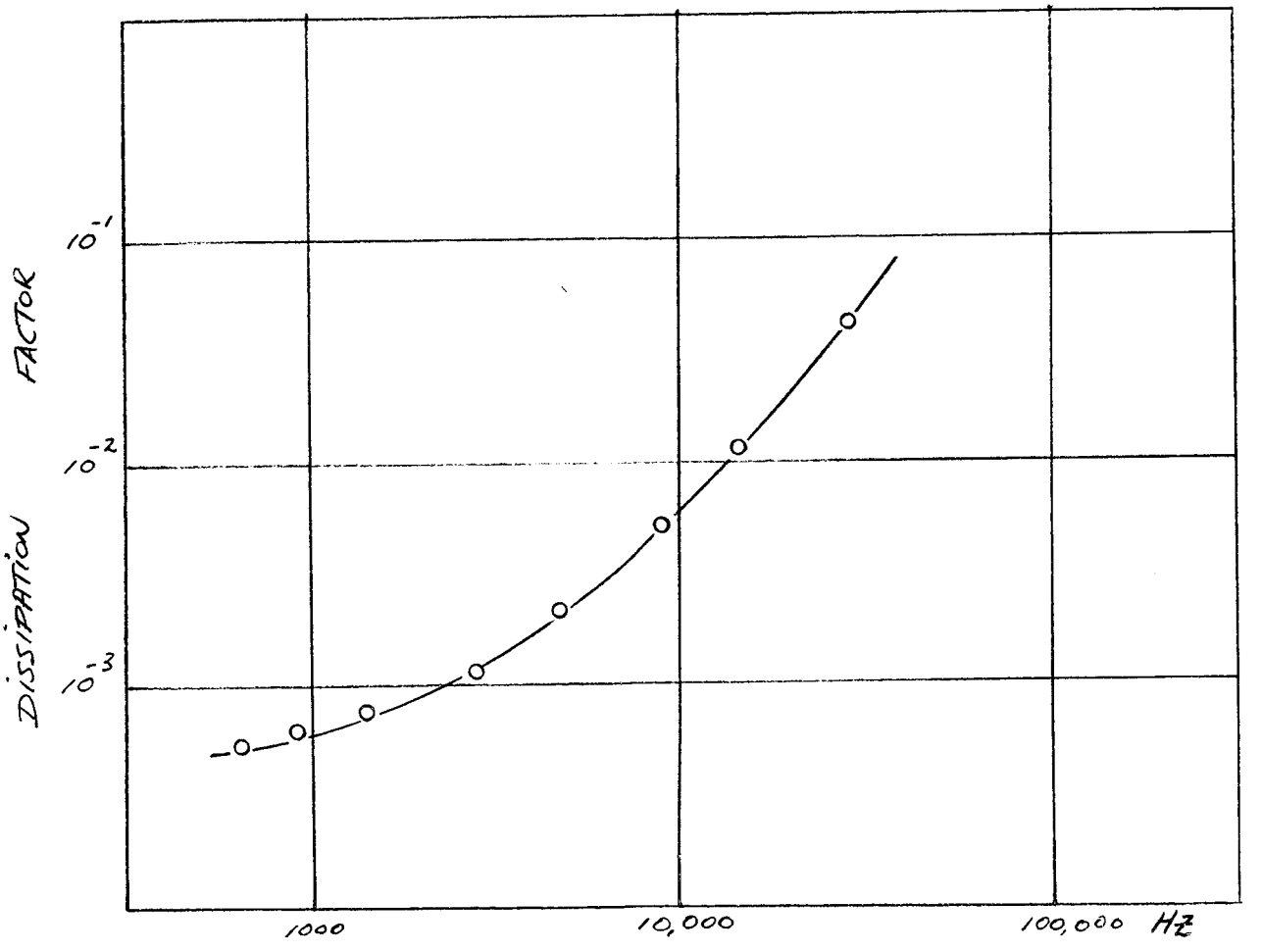

Figure 2 Dissipation factor vs frequency for polymer dielectric thin film capacitor

at much higher current levels, but this is readily accomplished with polymer films which have more charge transport capacity. The current levels approach the microamp to milliamp range in this new configuration, indicating a much greater density of bulk sites which take part in Schottky or Pool-Frenkle processes. The development has lifted the entire concept of thin-film MPS devices using tunneling and depletion-layer saturation to a more general set of behaviors. These have higher current characteristics, several more mechanisms which can produce discontinous I-V characteristics and more opportunities to discover transducer behaviors in the processes and materials. If the tunneling process is not the only one which can be used, the requirement of extreme thinness (less than 180 Å) can be relaxed to insure greater yield and voltage breakdown limits. This development occured late in the second six months, so the entire scope of this has not become clear.

This phase of the program has developed into a much broader investigation, so that more problems of fabrication technique are slowing down the total effort. This is largely a matter of manpower, not facilites or ideas. More effort, meaning more manpower placed in this area, could be justified. Digital Transducer ideas have grown to a very promising number, with enough variety to warrant optimism about the eventual commerical value of the results of this research.

SILICON NITRIDE FILM RESEARCH

An essential part of the MIS digital transducer concept is that active dielectric materials will provide a characteristic response to external stimuli. A basic digital behavior in the MIS thin film configuration is discussed in Vol. I. The hoped-for digital transducer will combine the two separate ideas. Dielectric materials which exhibit a variety of charge transport mechanisms are being studied to supply the needed characteristics. Largely as a training

in exotic dielectric materials research we have partially supported a project on films of Si_3N_4 . Volume IV of this report describes the successful effort in detail. It is an intermediate step in the design of new and active dielectric materials.

II. CHEMICAL VAPOR DEPOSITION

A. INTRODUCTION

Dielectric materials may function in several roles in digital devices. The purpose of investigating them is to find classes of behavior which are compatible to tunneling digital transducers by having a characteristic response to an external stimulus. The development of methods for the chemical vapor deposition of uniform and stable thin films of dielectrics with a wide range of characteristics, especially parametric dielectric constants, is the objective of one phase of program. High dielectric constant materials offer the advantage of higher capacitance without the necessity for larger areas or thinner films which lead to pin holes and device failure. The small volume of active material in a thin film transducer can be compensated for if the response is a very sensitive one. A literature search reveals several methods for producing thin films of materials having a high dielectric constant ($\varepsilon > 100$) Chemical vapor deposition (a generalized title for epitaxy) offers the most flexible approach of all the available ones.

To be compatible with integrated circuits, a thin film capacitor must satisfy several criteria: Low dissipation factor, voltage insensitivity, nonpolarity, high stability during integrated circuit processing and high yield. Many materials currently used as capacitor dielectrics for thin film microcicuits exhibit low dielectric constants or low breakdown voltages such as SiO_2 ($\varepsilon = 4.8$, breakdown = 5×10^6 v/cm) and Si_3N_4 ($\varepsilon = 6.2$, breakdown = 1×10^7 v/cm). The pyrolysis of metal alkoxides constitutes the basis for this chemical vapor deposition (CVD) technique. Titanium oxide looks promising for a beginning because much bulk data exists, its properties are desirable and

appropriate source chemicals are readily available. Thin films of other titanium compounds offer desirable dielectric properties. Although these materials have been manufactured in bulk form, technology is lacking for their manufacture in thin-film form.

The development of a technique for the preparation of thin films of materials having high dielectric constants would constitue an important step toward the extension of thin film capacitor technology to permit a wider range of applications for integrated circuits. Other dielectric applications include diffusion masking, isolation for contacts, and mechanical and chemical stabilization.

B. CHEMICAL VAPOR DEPOSITION

1. Basic Kinetic Considerations

A number of steps must occur for the overall deposition: diffusion of the reactant through the static layer adjacent to the substrate, adsorption onto the substrate, diffusion of the adsorbed species across the surface to active sites, the chemical reaction, deposition of the non-volatile products, desorption of the volatile products, and their diffusion away from the vicinity of the substrate. The first and last steps are generally not independent, since the diffusion rate of the reactants affects the diffusion rate of the products, and stoichiometry influences the two steps of the reaction, and both affect the chemical reaction rate. The complex intermediate steps normally involve surface and gaseous reactions as well as simultaneous adsorption-desorption and nucleation processes. Any of the above steps may determine the rate of deposition, and relative importance of each of these steps in determining the rate should vary with the deposition temperature. In the low-temperature

range (<350° C) the deposition rate depends predominately on the chemical kinetics. That is, the deposition rate is relatively insensitive to the flow except at very low flows, but is strongly dependent on deposition temperature. In the high temperature range (<350° C) the major limiting factor is gas-phase diffusion. In this case, the rate of deposition depends strongly upon the geometry of the deposition system and upon the flow. The deposition rate is relatively insensitive to the temperature.

In establishing the overall kinetics of the deposition, one needs to treat the experimental data so as to evaluate the relative influence of the diffusion flux and the chemical kinetics, and to develop expressions for calculating their simultaneous influences on deposition rate. The thermodynamic section discusses these considerations more fully.

2. Vapor Plating Requirements

The general requirements for any gas plating reaction may be summarized as follows:

a. the reactants must be in the gaseous or vapor state,

b. the product to be deposited must be condensible at the substrate, and

c. the by-products formed in the reaction chamber must be sufficiently volatile to allow their ready removal.

In addition to these general requirements, the thermodynamics and kinetics of any particular vapor plating reactions impose restrants upon the deposition temperature and reaction concentrations which are unique to the reaction under consideration. Another section of this report discusses this requirement.

3. Deposition Apparatus

A versatile apparatus allows its use for a number of vapor plating reactions..

Reactions generally differ only in detail---source gases, concentrations, temperature, flow rates. Such a general purpose CVD apparatus will provide a means for the regulation of the reactant concentrations at the plating zone, a means of dispersing the reactant goods evenly over the substrate, and a means for the regulation of the substrate temperature.

Figure 3 illustrates such an apparatus. The temperature sensor is an infrared radiation pyrometer which is focused through a quartz window onto the substrate surface. An rf induction coil surrounding the quartz deposition chamber heats the graphite susceptor. The water jacket surrounding the reaction chamber keeps the quartz wall temperature low enough to limit the deposition to the susceptor and substrate. Pressure regulators, regulating valves, and flow meters provide the necessary regulation and control. Gas washing bottles serve as vaporizers for the reactants which are in liquid form at room temperature. Stainless steel lines and valves help insure purity of the deposit.

4. Advantages of Chemical Vapor Deposition

Silicon oxides have been the most widely used dielectrics in microelectronics in the past. Silicon dioxide grows thermally on silicon. Silicon monoxide evaporates readily in a vacuum chamber. Thermal oxidation disadvantages include:

a. Film not structurally perfect
b. Film purity not perfect
c. High temperature required
d. Abnormal transition regions at metal-insulator or semiconductor - insulator interface.
e. Composition of film limited by substrate.

The main objections really stem from the fact that years of technological development have yet to make these materials perform as satisfactorily as device reliability and performance criteria demand.

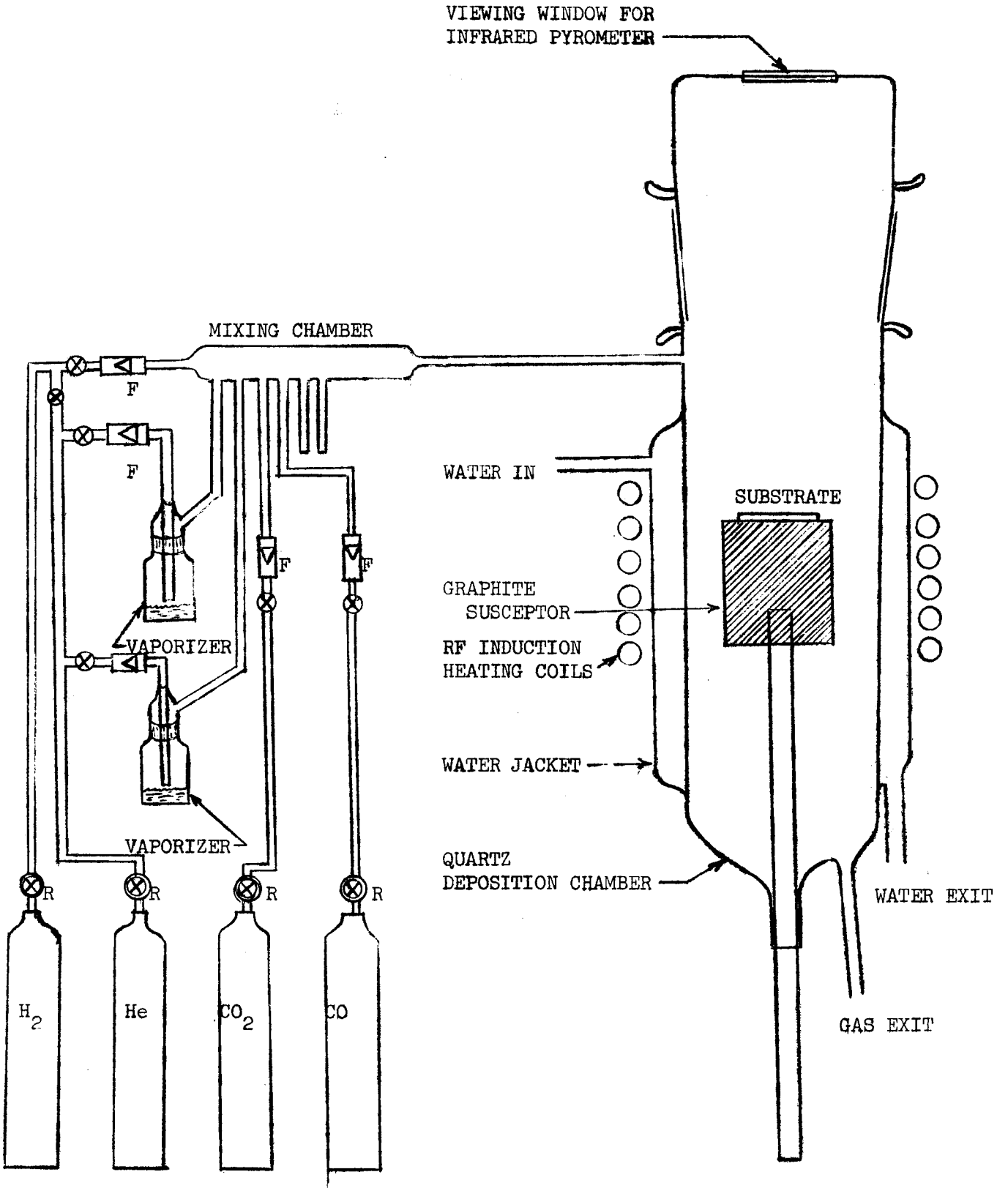

FIGURE 3 DEPOSITION APPARATUS

Physical vapor deposition, including dc or rf reactive sputtering has the disadvantage of limited versatility in the composition of the deposited film. In addition the films formed by this technique do not appear to be as smooth as those formed by CVD.

Chemical vapor deposition offers several advantages over other methods. Some advantages which justify the study and development of CVD of oxides from organic presursors are:

a. Much versatility is possible since films can be deposited on metals, semiconductors or other dielectrics
b. The oxide film should be very homogeneous since the reactant emanates from a source with preservable integrity.
c. Water vapor need not be present in the deposited film.
d. A sharper, cleaner, interface can be expected since inter-diffusion can be minimized.
e. The composition of the film can be controlled independently of the composition of the substrate.
f. The processes involved generally can be carried out at lower temperatures than those required for deposition from inorganic systems.
g. The reactant and product vapors of the organic systems are usually less reactive and corrosive than those of the inorganic systems.
h. Coating thickness can be varied, and fairly well controlled, over a wide range.
i. By reason of the very large number of available chemical reactions, chemical vapor deposition is seem to be a process of great versatility and flexibility.
j. The organic reactions are more suitable for the preparation of high-purity oxides.

5. Thermodyamics

Thermodynamics provides a powerful tool for analyzing new chemical transport processes. If the various thermodynamic factors are known or can be estimated with reasonable accuracy, a complete analysis of the process can be made and, when combined with kinetic and transport information, should lead to the determination of the optimum operating conditions.

The free-energy fuction provides a true measure of the chemical affinity of a reaction. The free-energy change in a chemical reaction is defined as

ΔF = F (products)- F (reactants). When the free energy change is zero, the system is in a state of equilibrium. When the free-energy change is positive for a proposed reaction, net work must be put into the system to effect the reaction. When the free-energy change is negative, the reaction can proceed spontaneously with the accomplishment of net work.

For processes occurring at constant temperature and constant pressure:

$$F = H - TS$$

The free energy F is equal to the difference in enthalpy or hear content H of the system at constant pressure and the product of the system temperature T and the entropy S.

The deposition process depends on the decomposition of the vapors of organometallic compounds. This decomposition takes place at atmospheric pressure in an oxidizing atmosphere containing H_2O to control the stoichiometry of the resulting oxide. The oxygen is introduced in the form of water vapor generated by the reaction.

$$H_2 + CO_2 + CO \qquad (1)$$

at the substrate. This reaction is not surface catalyzed and proceeds readily in the forward direction provided the temperature of the gases is greater than $800^{\circ}C$. The water-gas reaction is incorporated primarily to reduce the premature hydrolysis of the organometallics since they would react with any water vapor that exists in the vapor space forming finely suspended alkoxides. Thus it is essential that all components retain their individual identities until they reach the substrate where they spontaneously react.

The research program at The Electronic Materials Research Laboratory has begun with a study of the vapor deposition of TiO_2. This can be

accomplished by the above reaction plus either a metal halide such as titanium tetrachloride $TiCl_4$, or an organometallic such as tetraisopropyl titanate, $Ti\ (OC_3H_7)_4$. The reactions that follow (1) above are:[37]

$$TiCl_4 + 2H_2O \rightarrow TiO_2 + 4HCl \qquad (2)$$

or

$$Ti\ (OC_3H_7)_4 + 2H_2O \rightarrow TiO_2 + 4CH_3CHOHCH_3 \qquad (3)$$

The organometallic appears most suitable for reasons enumerated above. The TiO_2 will be deposited on a quartz substrate between two layers of a metal such as molybdenum or platinum. The insulating film will them be studied to determine the electrical, physical, chemical, and crystallographic properties and to determine the deposition conditions which yield the best films. Titanium dioxide has a dielectric constant of approximately 80. Having established the optimum conditions for the deposition of TiO_2 the program will then begin to investigate other titanates and mixtures which will yield improved dielectric properties. One such material of this type is lead titanate, $PbTiO_3$. The alkyl derivations of lead have sufficient volatility and stability to be very promising for such an application. Tetraethyl lead, $(C_2H_5)_4Pb$, and tetraisopropyl titanate form the desired $PbTiO_3$ which has a dielectric constant of from 250-300[75]. It is expected that barium titanate and strontium titante would not be as suitable for formation by this technique as other compounds because the organometallic compounds of barium and strontium do not form covalent bonds and also the volatility of these compounds is low. Also some of these organometallics have low stability. Lead titanate is an attractive dielectric for thin film capacitors because it is known to have in bulk form a high dielectric constant and a curie temperature considerably higher than that of barium titanate.

The lead and titanium compounds above are liquids at room temperature and have sufficient vapor pressure to permit the rate of delivery of the

respective gas to the reactor to be controlled by regulation of the flow of hydrogen over the liquid rather than bubbling through the liquid. This is desirable in order to prevent the formation of spray droplets which may collect downstream producing a variable and too concentrated a plating atmostphere. They may also tend to nucleate growth defects on the surface of the substrate.[6]

For the reactions under consideration (Equations 2 and 3) the standard free energies are negative at room temperature but the reactions will not occur at this temperature because they are dependent upon the water vapor being produced by the water-gas reaction (Equation 4). The standard free energy for this reaction shown in Figure 4 gives evidence that the reaction proceeds spontaneously only at temperatures above 800°C.[36,17]

Work on various metal-organic compounds presented at a Symposium on Metal-Organic Compounds at the Miami meeting of the American Chemical Society in April, 1957, appears in book form[13]. From papers presented by Herman and Beachman of the National Lead Co. and Hasham of duPont at this conference and from work of Bradley[14], Brill[15] and other published data[16] one gains an insight into the chemistry of titanium organic compounds.

The alkyl titantes may be considered the esters of orthotitanic acid [$Ti(OH)_4$] in which the four hydrogens of that hypothetical acid are replaced by four alkyl groups. Thus $Ti(OR)_4$ is the general formula for an alkyl titanate, R representing the alkyl group.

On exposure to water, moist air, or substances containing water or hydroxyl groups the alkyl titantes hydrolyze. Isopropyl titante hydroyzes very rapidly, sec-butyl titanate hydrolyzes rapidly, butyl titanate hydrolyzes, and 2-ethylbutyl and 2-ethylhexyl titanates hydrolyze relatively slowly thus affording the researcher an opportunity to vary rates of hydrolysis as well as the type of hydrolysis product. The extent and rate of

STANDARD FREE ENERGY OF REACTION

$$CO_2 + H_2 = H_2O + CO$$

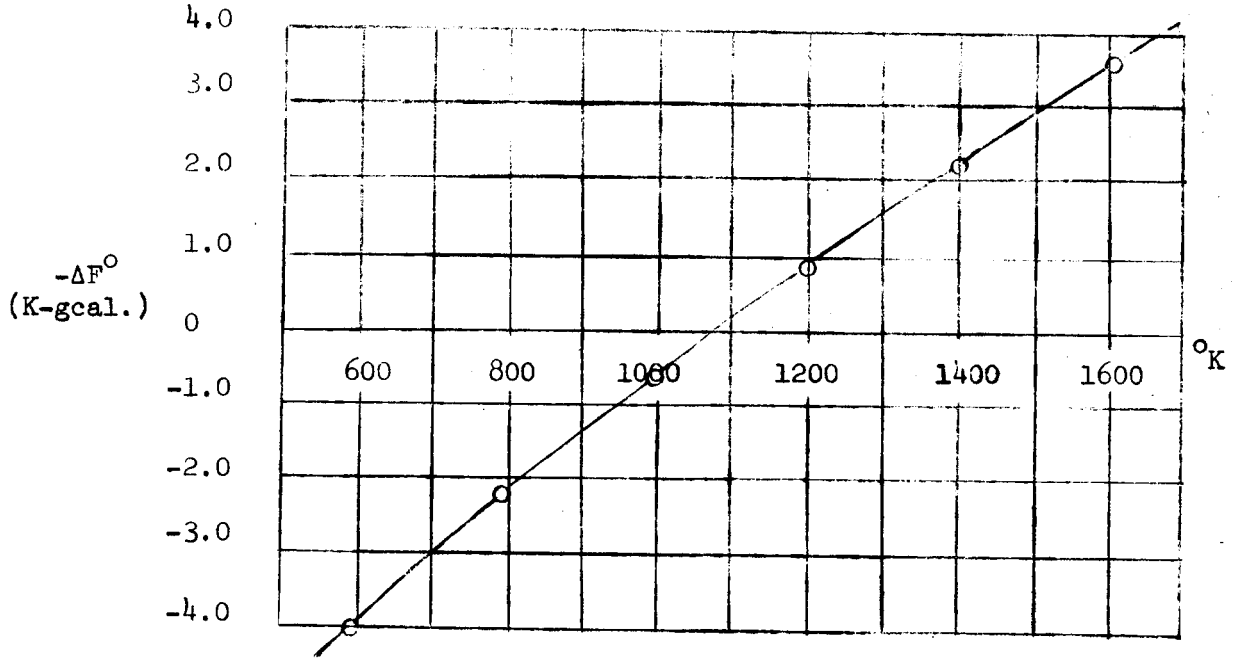

TEMPERATURE °K

FIGURE 4

the reaction are mainly dependent upon the ratio of water to alkyl titanate. In all cases the eventual result of complete hydrolysis is the formation of titanium hydrate and released alcohol. The mechanism is believed[15] to involve the formation of an intermediate complex between the ester and water. The reactions are:

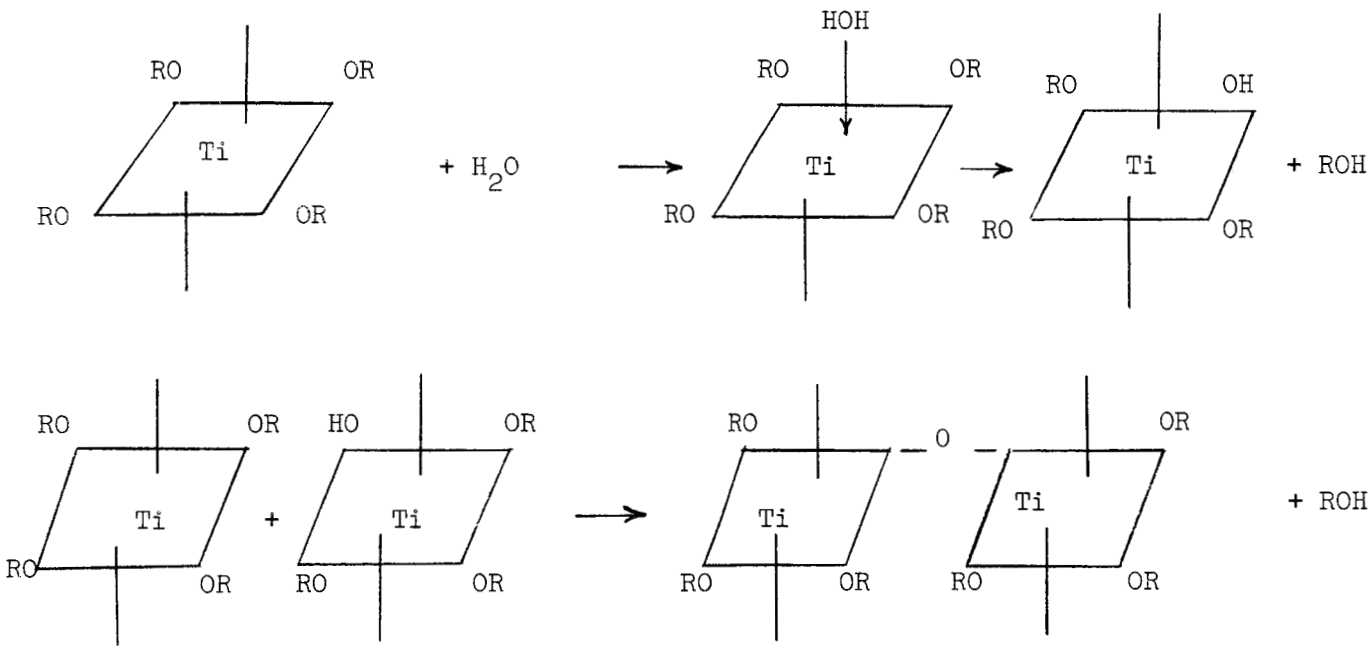

The hydroxyl ester cannot be isolated since it immediately reacts to give the dimer. The hydrolysis proceeds stepwise as shown in the following reaction:

$$x(RO)_3TiOTi(OR)_3 + xH_2O \rightarrow 1(-Ti(OR)_2O-)_{2x} + 2xROH$$

and continues as follows:

$$(-Ti(OR_2)O-)_x + xH_2O \rightarrow xTiO_2 + 2xROH$$

giving as the end result a clear amorphous film of TiO_2. As pointed out previously the water gas reaction (equation 1) will make this reaction more

controllable and prevent deposition of the TiO_2 prematurely before reaching the substrate.

The alkyl titanates when heated pyrolyze to yield relatively hard glassy products[16]. In the case of butyl titanate, the reaction can be illustrated as:

$$2(C_4H_9O)_4Ti \xrightarrow[\Delta]{300^\circ C} (C_4H_9O)_3TiOTi(OC_4H_9)_3 + C_4H_9OH + C_4H_8$$

The primary decomposition products of isopropyl titanate seem to be propylene, isopropyl alcohol, and titanium dioxide (Haslam[13]).

Thus TiO_2 films may be deposited by pyrolysis by using a carrier gas to convey tetraisopropyl titanate vapor to a hot surface (500-600°C) or by hydrolysis utilizing the water-gas reaction and a hot surface (800-1000°C).

Regarding the second phase, the production of mixed titanates, tetraethylead--commonly abreviated to the TEL--is a simple organometallic compound of moderate chemical reactivity. TEL is very stable at room temperatures, but on heating it undergoes an exothermic dissociation, giving a complex of reaction products. Milde and Beatly[13] point out the TEL undergoes interchange reactions with other lead alkyls and with certain other metal alkyls to give a mixture of products. Other recent work[34] indicates the feasibility of forming mixed titanates by chemical vapor deposition.

These calculations only represent the overall reaction and only show that the reaction is thermodynamically possible. They do not show us the rate or mechanism by which each system approaches equilibrium for this cannot be readily predicted by purely theoretical considerations. To establish the reaction kinetics for each vapor plating system recourse to direct experimentation is necessary. The results of thermodynamic calculations should be interpreted with due caution because they may be based on incorrect data

or may be unattainable because of kinetic factors. Powell, Oxley, and Blocher[6] cite examples of processes which are impossible thermodynamically and which do work.

Thermodynamics therefore provides a powerful tool for analyzing the feasibility of a given deposition process, but from a practical viewpoint the process is frequently also governed to a large extent by kinetic factors. Only a careful experimental program can properly evaluate a specific chemical system.

III. ANALYSIS OF METAL-POLYMER-SEMICONDUCTOR DEVICE CAPACITANCE

A. INTRODUCTION

The ultimate success of a tunneling MIS digital device will be dependent upon an understanding of the charge storage and transport processes. The thin film metal-insulator-semiconductor capacitance, taking into account the tunneling and Schottky emission current flow, is discussed in this section. Previous research on MOS devices has been less complicated by lack of significant flow of charge through the insulator. In this research on digital devices, however, the additional complication must be considered. Traps or recombination centers in the polymer insulating thin layer may be charged by the current passing through it. As more electrons pass through, the probability increases that the traps and recombination centers are filled. A small increase in MPM (metal-polymer-metal) capacitance due to the increase of bias voltage is believed to be the result of the increasing charge trapped in the insulating layer.

From the measurements reported in Vols. I, III and IV, it is now apparent the MPS capacitor needs additional features to its model than available for the MOS structure with a thick (> 1000 Å) insulating layer. This chapter of the report is a survey of the existing models, with the direction of our own effort indicated. The sections B-H review the MOS capacitor theory, sections I and J discuss the manner in which the charge trapping and transport may be introduced to modify the MPS system model.

B. CARRIER DENSITIES AND BAND MODEL FOR AN IDEAL SEMICONDUCTOR SURFACE

The energy-level diagram for a semiconductor surface can be shown

as follows:

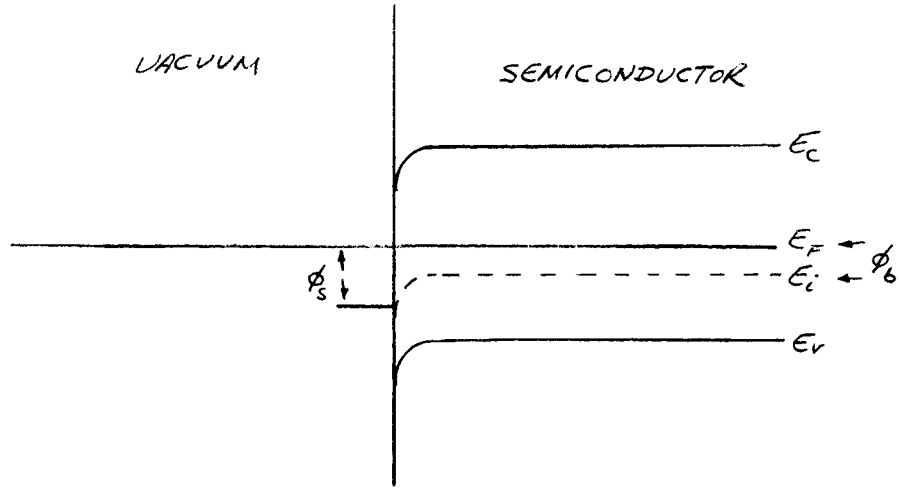

Fig. 5. Energy-level diagram for a semiconductor surface

Referring to the above diagram, the concentrations of free electrons, n, and holes, p, in the semiconductor in thermal equilibrium are:

$$n_b = n_i e^{(E_f - E_i)/kT} = n_i e^{q\phi_b/kT}$$

$$p_b = n_i e^{(E_i - E_f)/kT} = n_i e^{-q\phi_b/kT}$$

$$n_s = n_i e^{q\phi_s/kT} = n_b e^{q(\phi_s - \phi_b)/kT}$$

$$p_s = n_i e^{-q/kT} = p_b e^{-q(\phi_s - \phi_b)/kT}$$

where n_b, n_s, p_b, p_s are the bulk and surface electron and hole concentrations respectively.

E_i = intrinsic Fermi energy

$$= 1/2(E_c - E_v) + e/4\ kT\ \ln(\frac{m_h^*}{m_e^*})$$

m_h^*, m_e^* are the effective mass of hole and electron.

The potential, with respect to bulk potential, at any point in the semiconductor, is given as $V = \phi - \phi_b$.

$$\text{Let } u = \frac{q\phi}{kT}$$

$$\text{and} \qquad v = \frac{qV}{kT}$$

The electron and hole densities at every point can be expressed as

$$n = n_i e^{u} = n_b e^{v}$$

$$p = n_i e^{-u} = p_b e^{-v}$$

V_s and ϕ_s are convenient means of classifying the surface conditions. If $\phi_s > 0$, the surface is n-type, and if $\phi_s < 0$, the surface is p-type. When the sign of V_s is opposite to that of ϕ_b and $V_s \geq 2\phi_b$, an inversion layer is formed at the surface, and if $V_s < 2\phi_b$, a depletion layer will be formed. If $V_s < 0$ for p-type material or $V_s > 0$ for n-type material an accumulation layer or an enhancement layer exists at the surface. When $V_s = 0$, this is flat band condition.

C. SURFACE SPACE CHARGE DENSITY

The electrostatic potential, ϕ, within the semiconductor crystal is related to the charge density, ρ, in the crystal through Poisson's

equation. In one dimensional case

$$\frac{d^2\phi(z)}{dz^2} = -\frac{\rho(z)}{\epsilon_s}$$

Where $\epsilon_s = K\epsilon_o$, is the permittivity of the semiconductor, and $\rho = q(N_D - N_A + p - n)$. N_A and N_D are the acceptor and donor densities and p, n, are the free hole and electron densities.

By substituting $\phi = \frac{\mu kT}{q}$, $N_D - N_A = 2\, n_i\, \sinh u_b$, and $n - p = 2n_i \sinh u$, the Possion's equation takes the form as:

$$\frac{d^2u}{dz^2} = \frac{1}{\lambda_i^2} (\sinh u - \sinh u_b)$$

where λ_i, the Debye length of the semiconductor based on the intrinsic concentration n_i, is defined as

$$\lambda_i = \left[\frac{\epsilon_s kT}{2q^2 n_i}\right]^{1/2}$$

The boundary condition is $u = u_s$ at $z = 0$ and $u = u_b$ at $z \to \infty$.

The above equation may be integrated to give the electric field, ε, as:

$$\varepsilon = \pm \sqrt{2}\, \frac{kT}{q\lambda_i} [(u_b - u)\sinh u_b - (\cosh u_b - \cosh u)]^{1/2} \qquad (1)$$

The plus sign is to be used for $u < u_b$ and the minus sign for $u > u_b$.

Let $u = u_s$, the electric field at the surface is obtained as

$$\varepsilon_s = \pm \frac{kT}{q\lambda_i} F(u_s, u_b)$$

where

$$F(u_s, u_b) = \sqrt{2}\,[(u_b - u_s)\sinh u_b - (\cosh u_b - \cosh u_s)]^{1/2}$$

To determine the total charge per unit surface area, Q_{sc}, let $u = u_s$ and use Gauss' law to get:

$$Q_{sc}(u_s) = \epsilon_s \varepsilon_s(u_s) = \pm C_o\left(\frac{kT}{q}\right) F(u_s, u_b)$$

where $C_o = \quad_s/\lambda_i$, represents an "effective" semiconductor surface capacitance per unit area. An effective Debye length L, is defined as[77]

$$L = \left[\frac{\epsilon_s kT}{q^2(n_b + p_b)}\right]^{1/2}$$

It is this length which characterizes the width of the space-charge region.

If an inversion layer is present at the surface, the electric field is expressed in a different way[78]. For p-type material:

$$\varepsilon_s = \left(\frac{kT}{q}\right)\left[\frac{1}{\lambda^2(n_s - n_b)} + \frac{1}{\lambda^2(p_s - p_b)} + \frac{1}{\lambda^2(N_A - N_D)}\right]^{1/2}$$

where the λ's are the Debye lengths based on the concentrations indicated by their subscripts.

For sufficiently high surface potentials, the surface field is simply

$$\varepsilon_s \cong \left[n_s\left(\frac{2kT}{\epsilon_s}\right)\right]^{1/2}$$

and the total mobile charge in this inversion layer is given by

$$Q_{sci} = -\epsilon_s \varepsilon_s = -[2\, kT_s n_s]^{1/2} = -2\lambda_{ns} q_{ns}.$$

D. SURFACE SPACE-CHARGE CAPACITANCE

Since the net charge in the semiconductor surface changes with variations in the potential across the surface layer, a differential capacitance, C_{sc}, can be associated with the semiconductor surface. This capacitance per unit area is defined as:

$$C_{sc} = \left|\frac{dQ_{sc}}{dV_s}\right| = C_o \left|\frac{dF(u_s, u_b)}{du_s}\right|$$

where Q_{sc} is the net charge in the space-charge layer and C_o is the effective semiconductor capacitance per unit area. For silicon C_o is 4.2×10^{-10} f-cm^{-2} and for germanium it is 9.36×10^{-9} f-cm^{-2}.

This differential capacitance can be measured by superimposing a small a-c voltage upon the applied d-c bias. An example plot of this surface space-charge capacitance, normalized with respect to C_o, versus the normalized surface barrier heights, V_s, is shown in Fig. 6. There, u_b is chosen as 15 which corresponds to $n = 4.6\ 10^{16}$ cm^{-3}.

However, the measured capacitance may decrease as the frequency of the test signal increases, since the charge in the space-charge layer cannot change instaneously.

For depletion or accumulation layers, the charge fluctuations are produced by a flow of majority carriers through the bulk of the semiconductor,

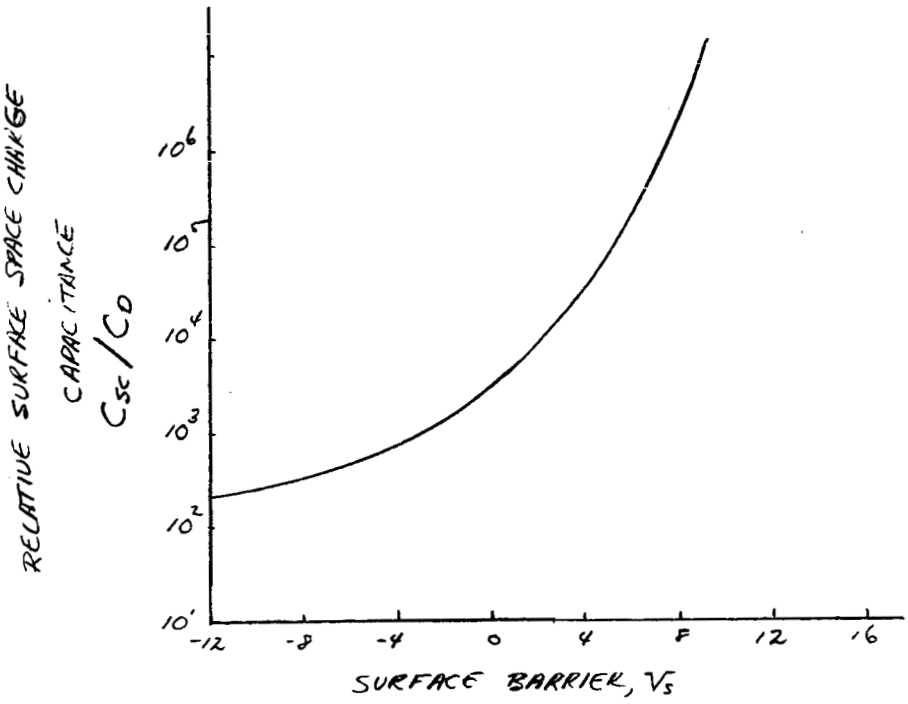

Fig. 6. Relative surface space-charge capacitance vs. surface barrier

and they will follow the applied voltage signal as long as:

$$\frac{1}{\omega} \gg \frac{\varepsilon_s}{\sigma_b} = \tau_r$$

where σ_b is the semiconductor bulk conductivity, and τ_r is the dielectric relaxation time of the semiconductor. For silicon, with a bulk conductivity of $\sigma_b = 10(\text{ohm-cm})^{-1}$, $\tau_r = 10^{-9}$ sec, it is clear that for all frequencies of practical concern the majority carriers will respond immediately. For inversion layers the time constant is much longer, typically 0.01 - 1 sec., and it is further described in the next section. Therefore, the differential capacitance is strongly frequency dependent.

E. FREQUENCY RESPONSE OF THE SURFACE INVERSION LAYER

The small-signal impedance and equivalent circuit model of metal insulator and semiconductor structures has been discussed and presented by several authors[81, 79, 80]. These discussions and presentations reflect the complexities of the mathematical results and are very difficult to use in practice. Hofstein and Warfield have presented an approximate analysis of the frequency response of the MOS capacitor when the surface layer is strongly inverted, with emphasis on the frequency response of the inversion layer itself[82]. Although this first-order one-dimensional model is not exact, it yields numerical values for the pertinent parameters of MOS capacitors which agree with experimental results to within an order of magnitude. When the surface layer is strongly inverted there are several sources which can supply the minority carriers required to charge the inversion layer[78]. Each of the sources can be represented by a resistance. This leads to the simplified equivalent circuit, shown in Fig. 7 on the following page.

R_d is associated with an electron diffusion current from the bulk, R_{go} with a volume-generated current within the depletion region, and R_{gs} is associated with a surface-generated current directly related to the surface states at the insulator-semiconductor interface, C_d is the capacitance of the depletion region. For p-type silicon (10 ohm-cm) at room temperature[78], a minority carrier lifetime of $\tau_n = 10^{-6}$ sec is taken. These resistances are: $R_d = 2 \times 10^8$ ohm-cm^2, $R_{go} = 5 \times 10^6$ ohm-cm^2, $R_{gs} = 1 \times 10^8$ ohm-cm^2. For this material $C_o = 10^{-8}$ f/cm^2, leading to inversion layer response times of $\tau_d = 2$ sec, $\tau_{go} = 5 \times 10^{-2}$ sec, $\tau_{gs} = 1$ sec. The response time of

the inversion layer will be

$$\tau_I = (\tau_d^{-1} + \tau_{gs}^{-1} + \tau_{go}^{-1})^{-1} = 0.645 \text{ sec.}$$

which corresponds to the response frequencies less than 2 cps.

A second-order model, which can explain certain "anomalies", such as hysteresis, has been proposed by Hofstein[83, 82]. The electrode inversion

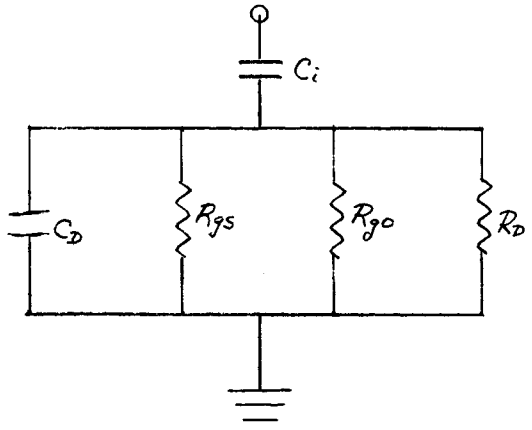

Fig. 7. Simplified equivalent circuit for determining the frequency response of the inversion layer.

layer is coupled to the bulk through a distributed RC network. A simple RC lumped circuit may be employed to approximate the distributed network as shown in Fig. 8. The frequency response of a p-type MOS capacitor has been investigated by Hofstein and Warfield. Their results showed a good agreement with the behavior predicted by this second-order model.

F. THE PRESENCE OF SURFACE STATES IN A REAL SEMICONDUCTOR SURFACE

The termination of the perfect periodicity of the crystal potential at a surface introduces localized allowed energy states, some of which are

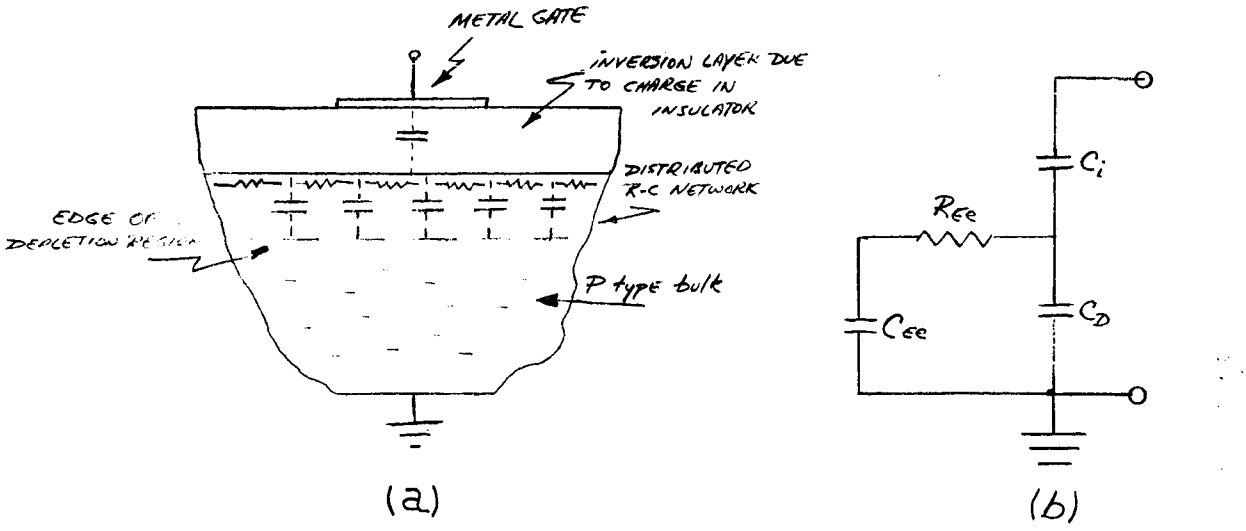

Fig. 8. (a) Two-dimensional model for explaining the anomalous frequency response observed in MOS capacitors

(b) Approximate equivalent circuit

in the forbidden gap. These are dangling or unsaturated bonds at the surface and may absorb gases and impurities as well as holes and electrons. The surface states are important because the fast states are mainly responsible for the generation and recombination of electrons and holes at the surface, and the slow states largely determine the surface potential by pinning the Fermi level at the surface trap level.

The probability of a trap site at energy E_t being occupied is given by[78]

$$f(E_t) = \frac{1}{1 + g\exp(E_t - E_f)/kT}$$

where $g = 1/2$ for acceptors and $g = 2$ for donors.

At equilibrium, the surface potential will adjust itself in such a way that the surface traps are filled in accordance with the above equation, and overall charge neutrality exists. This means the surface potential is such that it produces the necessary charge in the space-charge layer until neutrality exists. If Q_{ss} is the total charge in surface states, then, with no applied voltage:

$$Q_{ss} + Q_{sc} = 0.$$

G. SURFACE STATES CAPACITANCE AND FREQUENCY

There is a differential capacitance, C_{ss}, associated with change of charge in surface states. It is defined as:

$$C_{ss} = \frac{2Q_{ss}}{2V_s}$$

The total surface capacitance is then given by:

$$C_s = \frac{2Q_T}{2V_s} = C_{sc} + C_{ss}$$

where $Q_T = Q_{ss} + Q_{sc}$ is the total charge at the semiconductor surface. Thus, the semiconductor surface capacitance is a parallel combination of space-charge and surface-state capacitance.

Associated with the frequency response of surface states, the response

time of a trap, τ_c, can be defined. It is the mean time before a trap is filled at the surface. Based on a tunneling model, the trap time-constant for a single trap level is given by[84]:

$$\tau_c = \frac{e^{2K_o z}}{2\bar{v}(S_n n_s + S_p P_s)}$$

where $\bar{v}$ = the thermal velocity of electrons and holes. S_n, S_p = the capture cross section for electrons and holes, and

$$K_o^2 = \frac{2m^*}{\hbar^2} (W - E_c)$$

where m* is the effective mass, and W is the height of the potential energy barrier at the surface.

The frequency response, f, of a monoenergetic trap level localized at the interface is described by the dimensionless function:

$$f(\omega) = \frac{1}{[1 + (\omega\tau_c)^2]^{1/2}}$$

which represents the fraction of trapped electrons that can follow an applied signal of angular frequency ω. The phase delay associated with the frequency factor will add a resistive component to the surface-state capacitance.

H. METAL-INSULATOR-SEMICONDUCTOR CAPACITANCE

In this section the general expression for metal-insulator-semiconductor capacitance is derived by assuming: (a) the film is perfectly

insulating (no tunnel or space-charge-limited current flow), (b) there is no contact potential between the metal and the semiconductor, (c) the surface states are uniformly distributed spatially on the insulator, (d) the field is essentially uniform throughout the insulating layer. If a voltage is applied across the device, the electric field terminates on two different kinds of charges; the charge in the semiconductor space-charge region; and charge in the surface states. Let N_{ss} represent the density of occupied surface states per unit interface area for the particular value of ϕ_s (and V_a). The charge in the surface states is $Q_{ss} = qN_{ss}$.

The total charge, Q_T, per unit area at the semiconductor is:

$$Q_T = Q_{sc} + Q_{ss}.$$

Assume the insulating layer thickness is large compared to the Debye length in the insulator, the electric field within the insulator has the magnitude V_i/d_i, where d_i is the insulating layer thickness. By Gauss law:

$$|Qm| = Q_T = C_i V_i$$

where $C_i = \quad_i/d_i$ is the insulator capacitance per unit area.

The total capacitance per unit area of the MIS structure is

$$C = \frac{\partial Q_T}{\partial V} = C_i\left(1 - \frac{\partial \phi_s}{V}\right) = \frac{C_i C_s}{C_i + C_s}$$

The total capacitance corresponds to a series combination of the insulating layer and the surface capacitance.

Since the insulator capacitance is constant and assumed to be frequency independent, the frequency dependence of the MIS capacitance is completely determined by the frequency dependence of the semiconductor surface capacitance.

The complete functional form, including frequency dependence of the over-all capacitance, can be obtained if we rewrite the voltage across the device as[89]:

$$V = V_i + V_s = V_{ss} + V_{sc} + V_s$$

where $V_{ss} = \frac{Q_{ss}}{C_i} = \frac{qN_{ss}}{C_i}$

and $V_{sc} = \frac{Q_{sc}}{C_i}$

are the voltage equivalents of Q_{ss} and Q_{sc}.

The situation with V_{ss} is complicated and depends on the distribution of the surface states with respect to energy and position in the insulator $K_t(z,E_t)$. It can be shown that, in general[84],

$$\frac{\partial V_{ss}}{\partial V_s} = \frac{q^2}{C_i} \int_0^{d_i} \int_{E_{Vo}}^{E_{Lo}} K_t(z,E_t) g(z,E_t) [1+\omega^2 \tau_c^2(z,E_t)]^{-1/2} \left(\frac{\partial f}{\partial E_f}\right) dE_t\, dz$$

where

$$g(z,E_t) = 1 - \exp[-e^{-2K_o(z-z_m)}]$$

is a pseudo-Fermi-Function in the variable z.

The frequency dependence of MIS capacitance is implied in the frequency dependence of $\partial V_{ss}/\partial V_s$. Since the small-signal time constant, τ_c, depends upon the applied bias through V_s, the frequency dependence will be a function of the bias.

The MIS capacitance as a function of the surface barrier can be obtained by use of $V = V_{ss} + V_{sc} + V_s$. It is:

$$C(V_s) = C_i\left(1 - \frac{\partial V_s}{\partial V}\right) = C_i\left[\frac{(\partial V_{sc}/\partial V_s) + (\partial V_{ss}/\partial V_s)}{1 + (\partial V_{sc}/\partial V_s) + (\partial V_{ss}/\partial V_s)}\right]$$

The MIS capacitance with tunneling or Schottky emission current flow is quite complicated, and at present stage, no compact equation or formula can be found in the literature.

The first step to derive an equation for MIS capacitance, which takes the tunneling current flow, probably is to understand the conduction through the insulating layer.

I. CONDUCTION PROCESSES THROUGH INSULATING LAYER

Conduction through insulating layers can take place in various mechanisms. Two of those mechanisms are Schottky emission and tunneling. We will discuss these two mechanisms very briefly in this report. For detail and more complete information refer to Volume III.

1. Schottky Emission:

Is the potential barrier, $\Delta\phi$, in a metal-insulator interface is small, or if the temperature is high, there will be electrons in the metal with sufficient energy to pass over the barrier and flow into the conduction

band of the insulator. For a small applied field this flow of electrons or the current per unit area is given as,

$$J_z = \frac{1}{(2\pi)^2} \frac{2qm^*(kT)^2}{h^3} \exp(-\frac{\Delta\phi}{kT})$$

This is the Richardson equation as in the case of thermionic emission in a vacuum. At room temperature, and for ordinary insulators the current given by the Richardson equation is negligibly small. However, by applying high electric field the height of the barrier may be decreased and causes more thermionic carriers to flow over the barrier. Including the image force, the lowering of the barrier height by an applied field ε is given by:

$$\Delta\phi_{max} = [\frac{q^3\varepsilon}{4\pi\epsilon_i}]^{1/2} \qquad (\text{where } \epsilon_i = K_i\epsilon_o)$$

Inserting this expression into Richardson's equation one gets the Schottky equation as:

$$J_z = \frac{1}{(2\pi)^2} \frac{2qm^*(kT)^2}{h^3} \exp\left[-\frac{\Delta\phi - (q^3\varepsilon/4\pi\epsilon_i)^{1/2}}{kT}\right]$$

$$= 120 \frac{m^*}{m} T^2 e^{-1.15 \times 10^4(\Delta\phi/T_e)13.8\ \varepsilon^{1/2}/(K_iT)^{1/2}} \text{ amp/cm}^2$$

2. Tunneling: Tunneling is a quantum mechanical process, which says there is a finite probability that a number of electrons without sufficient energy can "leak" thrcugh the potential barrier. Refer to the following figure and apply WKB approximation[85] the probability P(E), that an

electron incident on and will pass through the barriers is

$$P(E) \simeq \exp\left\{ - \int_{z_1}^{z_2} [2m^*[\phi'(z) - E)]^{1/2} dz \right\}$$

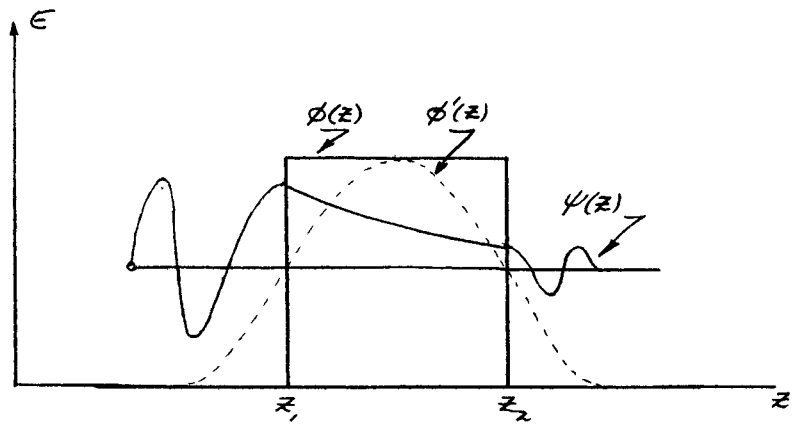

Fig. 9. One-dimensional tunneling

From the above equation we know the transmission probability is exponentially dependent on the thickness of barrier or insulator.

For a very thin insulating layer (say less than 200 Å) electrons can tunnel directly from a metal through the forbidden band into the conduction band of the other metal or semiconductor. For thicker insulator the tunneling probability is negligible, but an applied high electric field across the insulator can narrow the barrier and permit electrons to tunnel into the insulator conduction band. There are also tunneling processes which transport charge in and out of traps.

The tunnel current passing through the insulator can be calculated by evaluating the integral,

$$J_z = q \int N(E) \cdot f(E) \cdot V_z \cdot P(E_z)\, d\bar{k}$$

where E is the kinetic energy of the electron in the incident metal, measured from the bottom of the conduction band.

There have been many attempts to evaluate the above equation, but the complete solution cannot be obtained in analytical form. Approximate calculations have been made by most authors, yet it may be valid only in certain limits[86, 87, 90].

J. THE INSULATOR WITH TRAPS

Real insulators have large quantities of defects or impurities. Their effects are two-fold. First, each imperfection introduces one or more localized energy states. States which are empty in equilibrium may trap free excess carriers, removing them from the conduction process. Second, localized imperfections scatter free charge carriers, thereby reducing their mobility. This is particularly true if the states are electrically charged (ionized impurity scattering).

Consider the case of the tunneling current as a steady-state process. Under the application of the electric field, electrons from a large reservoir flow into the insulator. If the density of electrons is smaller than that of the traps, most of the electrons will be trapped, leaving only a small number of thermally excited free carriers. The ratio of free to trapped

charge, in the simplest situation, is:

$$\frac{n_c}{n_t} = \frac{N_c}{N_t} \exp\left[-\frac{\Delta E_t}{kT}\right]$$

where N_c = the density of states in the conduction band

N_t = the density of traps

ΔE_t = the ionization energy of the traps

As the voltage is increased and the number of carriers injected into the insulator becomes larger than the number of traps, the excess carriers remain free. It is therefore expected that the current through an insulator with traps will increase very strongly at a certain voltage, eventually approaching the value of the trap-free case. Any remaining difference is caused by a reduction of the mobility due to the ionized traps. One of the ideal data sets is shown in Fig. 10^{90}

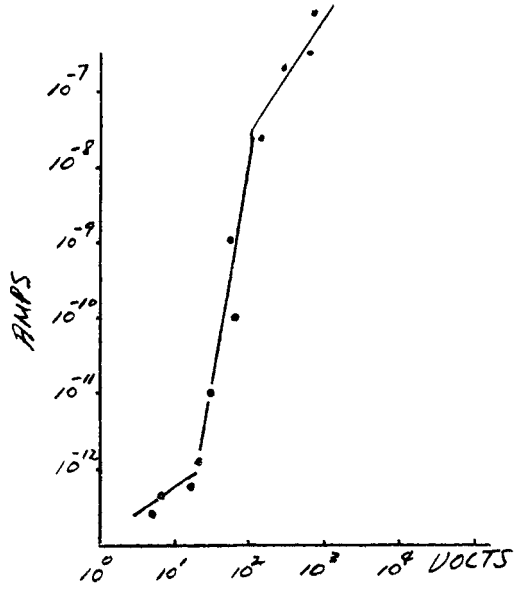

Fig. 10. Space-charge-limited current in a 5 10^{-3} cm-thick ZnS crystal

The filling or emptying of traps in the insulator will certainly affect the thin film capacitance reading. We have found out that the thin film MPM capacitance will increase as the bias voltage increases. This is probably because the charge trapped in the insulator has been increased as the current through the insulator increases. A frequency dependent MPM thin-film capacitance also has been observed in the laboratory. This might be caused by the frequency dependent characteristic of the polymer. Yet, the charging and discharging processes of these traps due to the frequency variation may possibly contribute the frequency dependent nature of the thin-film MPM capacitance. So far, no equations or detailed discussions about the bias voltage and frequency dependence thin film metal-insulator-metal capacitance can be found in the literature. The program for the next six months is, with experimental work, to develop an empirical equation which can be used to guide device modeling.

K. DISCUSSION

We have learned, through the previous sections of this report, that the thin film metal-insulator-semiconductor capacitance is the series combination of the dielectric capacitance and the surface capacitance. The semiconductor surface capacitance is in turn, a parallel combination of space-charge and surface-state capacitance. Equivalent circuits of the first-order and second-order model have been proposed and in certain cases they agree with the experimental results in magnitude. Yet, most of these equivalent circuits are derived by assuming that the thin film is perfectly insulating (no tunnel or space-charge-limited current flow) and is defect free.

We already knew that there is current flow in the insulating film when the MIM structure is biased with certain voltages. We also observed the increasing of capacitance by increasing the bias voltage. We believe that this increased capacitance was due to the excess charge carriers available to charge the traps in the insulating film. The current through the insulating film can be measured in the laboratory and it obeys the simple relation that $J = qNv_d$, where N is the carrier density and v_d is the velocity of the carrier passing through the film. Therefore, if we knew N we can calculate v_d and vice versa. The increased capacitance or the differential capacitance, $C = \frac{dQ}{dV}$ also can be measured in the laboratory. Therefore, dQ, the charge in traps can be calculated, and through the probability equation for filling a trap, the excess charge carrier density may be estimated. Thus, by the differential capacitance measurement we may define a velocity or mobility of an electron passing through an insulating film. It is worth noting that the electron velocity in passing through the insulator has not been discussed in any literature we have seen to date.

Many kinds of defects may exist in insulators and they can all influence the conduction properties, and as well as the capacitance in one way or another. Consider first the intrinsic defects. All common insulators have two kinds of intrinsic defects: a Frenkel defect and a Schottky defect. These defects and their relationship to impurities are responsible for ionic conduction.

Impurities are also a kind of defect. They may act as donors or acceptors. Excitation may be caused by photon absorption or impact ionization. Due to the inverse process the impurities may act as traps. They also reduce the mobility of the carriers, particularly if they are charged.

Another type of defect, which may be present in any kind of insulating layer, is a void or conglomeration of vacancies. They may adversely affect the properties of the layer in various ways. If the voids reach the surface they may be filled up with metal atoms during deposition of the film. They may increase the surface area, thereby increasing the problems due to absorbed ions. Finally, they reduce the breakdown strength of the layer because of their reduced dielectric constant.

In the literature discussing the metal-insulator-semiconductor structure, the space charge layer in the metal insulator interface has always been neglected. It was found that the thickness of the space-charge region in the metal, d_m is given as[78]:

$$d_m = \left[\frac{2}{3}\,\frac{E_m E_F}{q^2 n_o}\right]^{1/2}$$

For a typical metal $n_o = 10^{22}\ cm^{-3}$, $E_F = 10$ ev, the dielectric constant $k_m = 1$, then $d_m \simeq 0.84\text{Å}$. The maximum possible capacitance,

$$C_{max} = \frac{E_m}{2d_m} = 5.6\ \mu f/cm^2.$$

For a very thin film capacitor the metal space charge region capacitance should be taken into account.

From the above discussion we understand that the thin film capacitance is an involved research subject, especially for the MPS thin film capacitor which we are interested in. Recently, we have estimated that the effective mass of the electron in the polymer may be much less than the effective mass in a metal or semiconductor. Efforts continue to account for the observed behavior and to construct valid models for the phenomena.

IV. OPTICAL DIGITAL TRANSDUCER CONCEPTS

A. PHOTODIELECTRIC DETECTION TRANSDUCERS WITH GERMANIUM AND SILICON

Photo-induced changes in semiconductor carrier density have been studied largely as they affect the conductivity. The associated change in the real part of the complex dielectric constant has not been observed at room temperatures since the effect is masked by the presence of thermal carriers.[91]

Personnel from the Electronic Materials Research Laboratory, The University of Texas at Austin, have observed the photodielectric effect in Si, and Ge at $4.2^{\circ}K$. The experiments were conducted in superconducting resonant cavities where the photodielectric effect caused a significant increase in the resonant frequency. A typical value for the sensitivity is 20 KHz per milliwatt of 9000 Å radiation at a resonant frequency of 787 MHz for a P-type, Ge sample. All materials tested obey the classical expressions for the complex dielectric constant with a free-carrier contribution. Calculations show the recombination time for electron-hole pairs is less than 10^{-7} seconds, perhaps by several orders of magnitude. This means the bandwidth of the photodielectric effect is well above 10 MHz.

The transducer consists of a cavity with a semiconductor sample at a temperature low enough to suppress thermal carriers. Operation in liquid helium permits the cavity to have the very high Q's associated with superconductivity. Unloaded Q's in excess of 10^{7} are routinely fabricated in our laboratory. Such Q's give the resonator exceptionally high frequency stability. The optical receiver acts as a wide-band AM-FM converter, receiving an AM optical signal of low power and producing a corresponding FM microwave

output. A low-noise microwave amplifier is used with the resonator to make a stable oscillator. An embryonic photodielectric receiver consisting of a photo-tuned cavity and amplifier which forms a transducer-oscillator is studied. The oscillator output is a frequency in the GHz range which is swept through a few KHz at a rate determined by the signal frequency fluctuations of the light beam. The stable local oscillator (probably an identical oscillator to the transducer-oscillator except offset by a suitable frequency) is used in a heterodyne circuit prior to FM detection and output. In its final form the complete receiver would incorporate optical components to form an "Antenna" and an optical path to the photodielectric sample. The base frequencies of the transducer-oscillator and local oscillator would be kept stable, both relatively and absolutely, to any degree found necessary by suitable design or by incorporation of a reference frequency standard. The use of superconducting circuitry assures the frequency stability will be comparable to a quartz crystal oscillator.

A classical solution of the free electron in a sinusoidal electric field leads to a complex relative permittivity as given by Eq. (IV-1)

$$\frac{\varepsilon^*}{\varepsilon_o} = \varepsilon' - j\varepsilon'' \qquad \text{(IV-1)}$$

In a solid there is a change in the real and imaginary parts as given by Eg. IV-2, where n is the density of free charge carriers.

$$\frac{\varepsilon^*}{\varepsilon_o} = -\frac{ne^2\tau^2\,(1-\omega p^2/\omega^2)}{m^*\varepsilon_o\varepsilon_\ell[1+\omega^2\tau^2(1-\omega p^2/\omega^2)^2]} - j\frac{ne^2\tau/\omega}{m^*\varepsilon_o\varepsilon_\ell[1+\omega^2\tau^2(1-\omega p^2/\omega^2)^2]} \qquad \text{(IV-2)}$$

If the free charge is created by photons of energy hc/λ, Eq IV-3 is the free carrier density in a sample with effective volume V_s, conversion efficiency, α, and lifetime, τ_L.

$$n = \frac{\alpha\tau_L}{V_s(hc/\lambda)}\ \psi \qquad \psi \text{ in watts.} \tag{IV-3}$$

The resulting expression for the dielectric constant is given by Eqs. IV-4, IV-5 and IV-6.

$$\frac{\varepsilon^*}{\varepsilon_o} = (\varepsilon_\ell - \varepsilon_\psi) - j\,\frac{\varepsilon_\psi}{\omega\tau} \tag{IV-4}$$

where ε_ψ is the free carrier component and τ is the carrier relaxation time.

$$\varepsilon_\psi = \frac{e^2}{m^*\varepsilon_o\varepsilon_\ell(hc/\lambda)}\ \frac{\tau^2(1 - \omega_p^2/\omega^2)}{1 + \omega^2\tau^2(1 - \omega_p^2/\omega^2)^2}\ \frac{\alpha\tau_L}{V_s}\,\psi \tag{IV-5}$$

$$\frac{\varepsilon^*}{\varepsilon_o} = \varepsilon_\ell - K\,\frac{\omega_L\tau^2}{\omega(1 + \omega_L^2\tau^2)}\left(\frac{\alpha\tau_L}{V_s}\right) - jK\frac{\omega_L\tau/\omega^2}{(1+\omega_L^2\tau^2)}\ \left(\frac{\alpha\tau_L}{V_s}\right)\psi \tag{IV-6}$$

The presence of ε_ℓ accounts for the dielectric constant of the crystal lattice.

When the semiconductor sample is placed in a cavity, there occurs a perturbation in resonant frequency, $\Delta\omega$. The relative magnitude, is given by Eq. IV-7 in terms of the unilluminated dielectric constant, ε_D, multiplied by the ratio of energies given by the integrals. When the sample is illuminated, another frequency perturbation occurs which is determined by

the new dielectric constant, ε_L.

Equation IV-8 is the final expression for the change in resonant frequency, where G is the same ratio of integrals as in Eq. IV-7. The magnitude of G is a function of geometry only and can be evaluated by a room temperature experiment. A typical value is 0.03, which is a measure of the fraction of cavity energy contained in photodielectric sample.

$$\frac{\Delta\omega}{\omega} = \frac{(\varepsilon'_D)^2 - \varepsilon'_D + (\varepsilon''_D)^2}{(\varepsilon'_D)^2 + (\varepsilon''_D)^2} \quad \frac{\int_{\text{sample}} \varepsilon_o E^2 \, dvol}{\int_{\text{cavity}} (\varepsilon_o E^2 + \mu_o H^2) \, dvol} \tag{IV-7}$$

$$\frac{\delta\omega}{\omega} = \frac{(\varepsilon_L - \varepsilon_D)G}{\varepsilon_L \varepsilon_D} = \frac{\varepsilon_\ell - \varepsilon_\psi}{(\varepsilon_\ell - \varepsilon_\psi)^2 + (\varepsilon_\psi/\omega\tau)^2} - \frac{1}{\varepsilon_\ell} \tag{IV-8}$$

The photodielectric effect is a unique phenomenon that has several fundamental advantages over other methods of detection. When combined with high Q superconducting resonant cavities the need for optical local oscillators is eliminated, yet the inherent sensitivity of quantum detection is retained. The photoconductive effect is suppressed, which minimizes the noise associated with conductivity modulation and also modified the RC time constant dependence for detector bandwidth. The optimum resonant frequency would appear to be in the range of 0.9 to 4 GHz which is several times higher than needed to contain the information transmitted over most channels. This provides a distinct advantage to an AM-FM telemetry receiver

because the noise can be reduced by integrating the frequency change over many cycles of the resonant frequency to improve the signal-noise ratio. To the extent that this is possible, the equations presented above lead to the prediction that the photodielectric receiver can work well below the microwatt range of signal power, with the limit of detection set by noise in external electronic circuits. The ultimate sensitivity is the same as any quantum detector.

The opportunity to use an RF local oscillator is made all the more attractive with the availability of high Q resonators. Superconducting tanks and cavities can be shown to have Q's in excess of 10^7, and for the simpler configurations of high frequency cavities the Q's can readily exceed 10^8. The local oscillator then has no need to use a quartz crystal which would have both lower Q and much lower resonant frequency. This advantage over the present start-of-the- art in oscillator design allows the frequency excursion to be much smaller since the short-term stability of the system will be higher.

The gain-bandwidth product of a photodielectric receiver is a complex function of material properties and system configuration. Gain of a photodielectric detector is proportional to the ratio, $\frac{\delta\omega}{\omega}$ which is the carrier frequency change per unit of optical power. For low values of ψ, Eq. IV-8 can be simplified to

$$\delta\omega = \frac{\omega G}{\varepsilon_\ell^2}\,\varepsilon_\psi \qquad \text{(IV-9)}$$

and substituting for ε_ψ

$$\delta\omega = \frac{\omega K G}{\varepsilon_\ell^2}\left\{\frac{\omega_L \tau^2}{(1 + \omega_L^2 \tau^2)}\right\}\left(\frac{\alpha \tau_L}{V_s}\right)^\psi \qquad \text{(IV-10)}$$

The term in brakets is the gain coefficient which summarizes the characteristics of the device in terms of its resonant frequency, geometry, material properties and optical wavelength. The photodielectric material properties are reflected in its relaxation time, dielectric constant, band gap, sample volume, surface condition, density and types of impurities, and lifetime. The dimensionless constant,

$$e^2 / \varepsilon_o hc = 1.455 \times 10^{-2}$$

Bandwidth of the photodielectric transducer can be shown to be limited by the semiconductor free carrier lifetime and the time necessary to propagate the transducer's response.

Consider an impulse of optical power incident on the detector. It is assumed that zero time is required for a photon to enter the semiconductor and create an electron-hole pair. If the light is extinguished instantaneously, the frequency will decay to zero with an exponential dependence since the created carriers recombine according tc

$$n_\psi = n_{\psi o} E^{-t/\tau_L}$$

The frequency versus time will thus be given by a proportional expression since frequency varies linearly with n_ψ in the low light level region.

The ultimate response of $1/\tau_L$ can be achieved only under low circuit noise conditions. If noise is present, a time of integration of the detector response (decision time) is necessary to be able to distinguish whether a signal is present or not. Only after this decision interval is completed can the information be changed and thus this time must be smaller than τ_L seconds

for ultimate detector frequency response.

The gain-bandwidth product, for those cases where bandwidth is dominated by lifetime, is now seen to be independent of lifetime. There remains a great variety of ways in which the gain, the bandwidth, and their product can be altered for an optimum design. One can clearly distinguish between the system requirements for ground-based and space installations and take separate paths toward a design of each. The application to digital telemetry would be attractive since the frequency shift of the transducer is readily used in digital systems.

B. THE PHOTODIELECTRIC EFFECT IN CdS

In materials such as Ge and Si, the photodielectric effect is a decrease in the real part of the complex dielectric constant which follows the optical excitation of the crystal. This decrease is a reflection of the dynamic response of free electrons. The effect is normally short-lived, however, due to free carrier lifetimes of the order of 10^{-9} sec in Si and Ge. It has been shown that these semiconductors are relatively wide-bandwidth and moderately sensitive detectors of light, suitable for detecting high frequency amplitude-modulated light. They would not be satisfactory transducers for steady, weak light, however.

Analysis showed that the gain-bandwidth product of a semiconductor photodielectric detector is a constant. Thus, sensitivity may be increased only at the expense of bandwidth. For steady, weak light, wide bandwidth is not needed, and sensitivity may be maximized. Since photoconductor gain is proportional to the free carrier lifetime, it would be expected that semiconductors with long free carrier lifetimes would tend to be sensitive optical detectors when operated in either the photoconductive or photodielectric mode.

Cadmium Sulfide is one of the most sensitive semiconductor photodetectors

at room temperature, and its speed of response is on the order of 10^6 slower than for Ge or Si. Thus it was hoped the photodielectric effect in CdS at low temperatures would be suitable to allow the use of this material in a slow but sensitive optical transducer.

Library research proved that CdS, and especially silver doped CdS (CdS:Ag), may in some cases be characterized by long free carrier lifetimes. Lambe[92] reported a photocurrent decay time of about 0.3 ms in CdS:Ag at 77°K. In another CdS:Ag sample at 77°K, Lambe[93] reports photocurrent decay times of about 10 minutes. Kulp[94] reported photocurrents which did not decay at temperatures below 208°K in a Na doped CdS crystal. Decay times greater than 1 minute in CdS at 276°K were observed by Bube[95]. Time dependence of capacitive decay in a capacitor with a ZnS-CdS powder dielectric, observed by Kronenberg and Accardo[96] had a two minute decay time at liquid air temperature. Matthews and Warter[97] reported photoconductivity decay times greater than 10^{-3} sec in CdS at 188°K. Many others observed similar long decay times. It must be remembered that lifetime and decay time are not the same, due to trapping effects. For example, a photoconductor with a density of n free carriers and n_t trapping sites has a response time given by

$$\tau_{on} = \left(1 + \frac{n_t}{n}\right) \tau_n$$

where τ_n is the free carrier lifetime, and thus the actual free carrier lifetime may be much less than the response time [A complete analysis of this problem is given by Rose[98]]. Even considering this difference between lifetime and response time, the free carrier lifetimes in CdS were still thought to be considerably longer than in Ge or Si at low temperatures.

In order to investigate the photodielectric effect in CdS at 4.2°K, a series of experiments was performed using the superconducting resonant cavity described in several recent publications for this laboratory[91]. With samples of CdS:Ag at 412°K the resonant frequency of the cavity proved to be a linear function of the integral of the photon flux. This behavior is shown in Figure 11 where it is noted that the slope of the curve is approximately proportional to the incident light intensity. Several features of this curve are noteworthy. First the effects of light were immediate and permanent. The frequency of the cavity began to drop as soon as light was applied and when the light was removed, no reverse in the frequency change was observed. Photoconductivity, on the other hand, does not behave in the same manner. It is seen than an appreciable time must pass before any optically produced current is observed, and then the current increases exponentially. When the light is removed, the photocurrent suffers a partial but incomplete decay.

C. EFFECTS OF VIBRATION IN CdS:Ag

It was accidentally discovered that part of the frequency drop could be reversed by the application of mechanical vibration. The corresponding response of the photocurrent in CdS:Ag at low temperatures is shown in figure 12. Here, the mechanical shock was created by rapping the test circuit soundly with a bottle; this could be classified as a relatively strong shock. It is seen that the effect of the shock was to quench the photocurrent. The application of several hours of weak light had been required to build the current up to the level indicated before the shock was applied, and the vibration was able to reduce the current considerably. Following the shock, the light remained on, the photocurrent continued to rise as if the time had been set back several hours. Thus, for either the photodielectric or the photoconductive effect, vibration has a quenching effect in some samples.

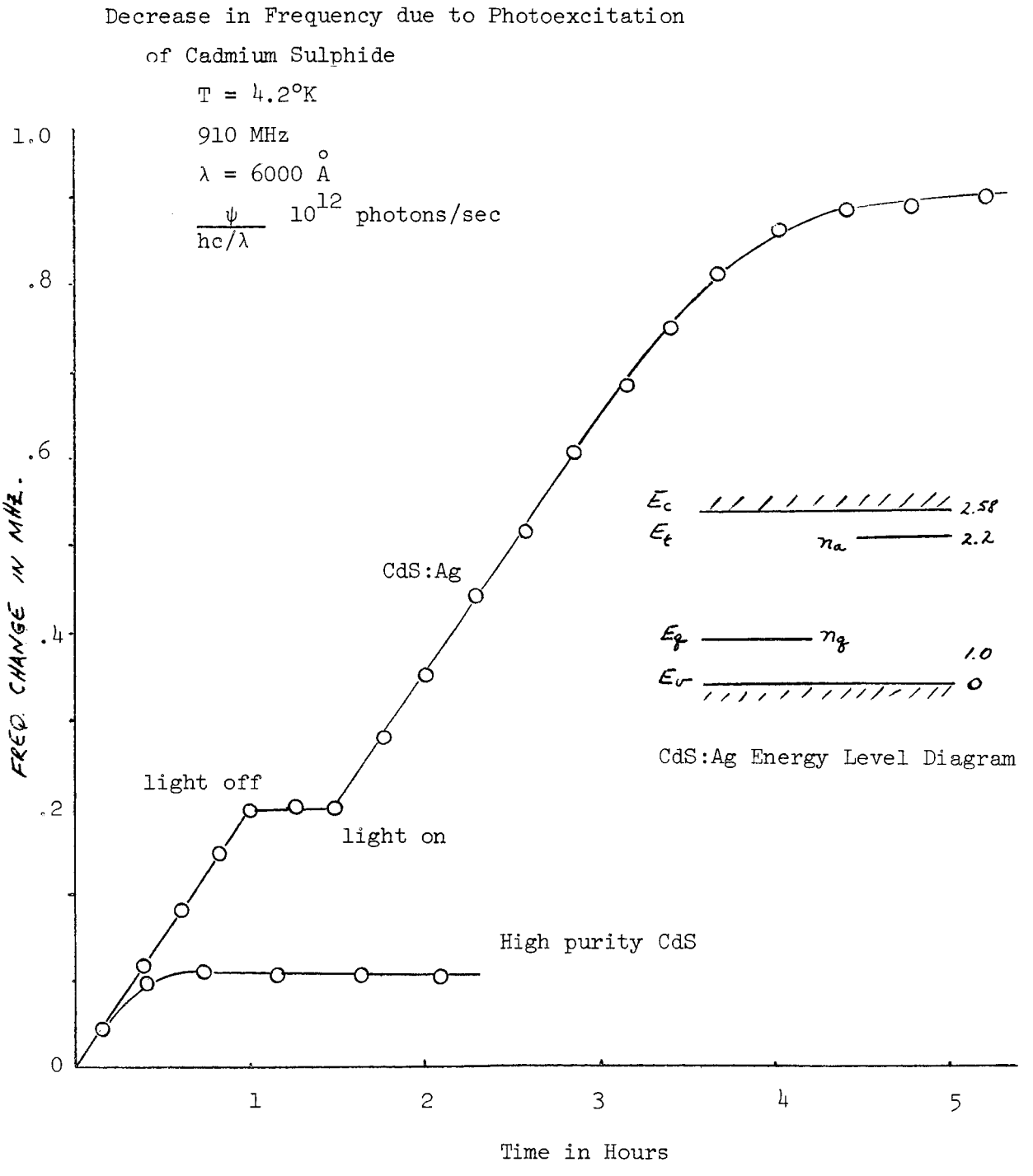

Fig. 11 Decrease in Frequency due to Photoexcitation of Cadmium Sulphide.

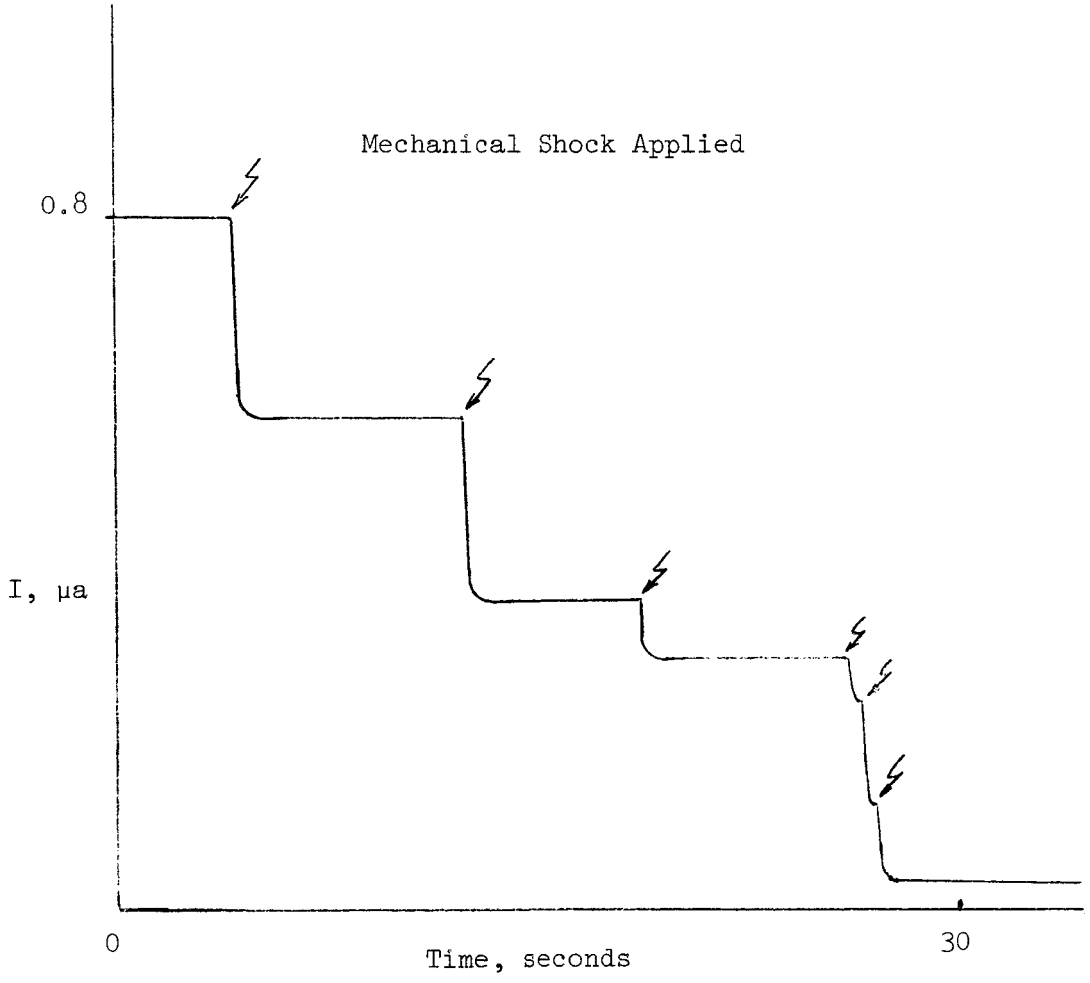

Figure 12 Response of Photocurrent in CdS:Ag at 77°K to Mechanical Shock of Random Intensity

V. BIBLIOGRAPHY

History and Review

1. Blicker, J. N. and J. H. Oxley, "CVD Opens New Horizons in Ceramic Technology", Bull. Am. Ceram. Soc. 41 (2), 81-85 (1962)

2. Glang, R. and S. Wajda, "Vapor Growth in Semiconductor Technology" Met. Soc. Conf. 15, 27-45 (1961)

3. Mountvala, A. J. and S. L. Blum, "Chemical Vapor Deposition for Electron Devices", Research/Development, 34 (July, 1966)

4. Podal, H. E. And M. M. Mitchell, Jr., "The Use of Organometallic Compounds in Chemical Vapor Deposition", Ann N. Y. Acad. Sci. 125 (1), 218-28 (1965).

5. Powell, C. F., I. E. Campbell, B. W. Gonser, Vapor Plating, John Wiley and Sons, Battelle Memorial Institute, Electrochemical Series (1955)

6. Powell, C. F., J. H. Oxley, J. M. Blocher, Vapor Deposition, John Wiley and Sons, Battelle Memorial Institute, Electrochemical Series (1966).

7. Sherwood, E. M. (Battelle), "Vapor Plating", Plating 52, 667-72 (1965)

8. Sherwood, E. M. and J. M. Blocher, Jr. (Battelle), "Vapo-Metallurgy: I Vapor Deposition [of Metals]: The First Hunderd Years", J. Metals 17 (6), 594-9 (1965)

Dielctric Review

9. Larssen, P. A., "Non-linear Dielectrics", Insulation p. 338 (May/June 66).

10. Von Hippel, A. R. et.al., "High Dielectric Constant Materials and Ferroelectricity"- Final Report No. AFCRL 6392 Contract AF 1906-6155, AD 404776 (Mar. 1963).

11. Von Hipple, A. R., "High-Dielectric Constant Materials as Capacitor Dielectrics", Technical Report 145, MIT Lab Insul. Res. (Dec. 1959)

12. Von Hipple, A. R. Ed., Dielectric Materials and Applications, Technical Press, MIT, Wiley, (1954).

Thermodynamics

13. American Chemical Society, Metal-Organic Compounds, A Collection of papers composing the Symposium on Metal-Organic Compounds of the Am. Chem. Soc. April, 1957. Adv. Chem. Ser. 23.

14. Bradley, D. C., R. Gaze, and W. Wardlaw, "Structural Aspects of the Hydrolysis of Titanium Alkoxides", J. Chem. Soc., 469 (1957).

15. Coutant, R. W., N. Albon, J. F. Miller, "Study of the Mechanisms of Pyrolytic Deposition" (Battelle), AD 468055 (August, 1965).

16. Brill, H. C., "Organo-titanates", TAPPI 38, No. 5, 141A-6A (1955).

17. Bulletin of the Titanium Pigment Corp. (National Lead Co.).

18. Dow Chemical Company, JANAF Thermochemical Tables (1960 to date).

19. Kaufman, H. C., Handbook of Organometallic Compounds, Van Nostrand Inc. New York, (1961).

20. Parks, Free Energies of Some Organic Compounds, N. Y.: Chemical Catalog Co. (1932).

21. Pitzer, K. S. and L. Brewer, Thermodynamics, (Lewis and Randall), New York: McGraw Hill, (1961).

22. Rochow, E. G., Organometallic Chemistry, Reinhold Publ. Co. N. Y. (1964).

23. Rossini, F. D. et. al., Selected Values of Physical and Thermodynamic Properties of Hydrocarbons and Related Compounds, Pittsburgh: Carneigie Press, (1953).

24. Schaffer, H., Chemical Transport Reactions, Academic Press, N. Y. (1964).

Recent Work in CVD

25. Arizumi, T. and T. Nishinaga, "Transport Reaction in a Closed Tube Process", Japan JAP 4(3), 165-72 (1965).

26. Barnes, C. R. and C. R. Gasner, "Pyrolytic Deposition of SiO_2 for 600°C Thin Film Capacitors", J. Electrochemical Soc. 110, 361(May 1963).

27. Black, J., D. Peterson, W. Brand, "Vapor Phase Deposition Methods for Metal Oxide Based Dielectrics", AD 450131. (Oct. 1964)

28. Black, J., D. Peterson, W. Brand, "Vapor Phase Deposition Techniques for Fabrication of Microelectronic Circuitry Thin Film Elements", AD 456793. (Jan. 1965)

29. Burcal, G. J. and J. D. Odenweller, "Research on Metal Organic Compounds for Vapor Plating Applications", AD 439594, (Jan. 1964).

30. Bylander, E. G., "Kinetics of Silicon Crystal Growth From $SiCl_4$ Decomposition," J. Electrochem. Soc., 109, 1171, (1962).

31. Callaby, Dr., "Surface Layer of $BaTiO_3$, JAP,37 2295, May(1966).

32. Campbell, I. E., personal communication Feb. 21, 1967.

33. Chu, T. L. and G. A. Grubec, "Silica Films by Chem-Transport, "Trans. AIME 223, 568 (1965).

34. Chu. T. L., C. H. Lee, J. R. Szedon, "Films of Silicon Nitride-Silicon Dioxide Mixtures", Presented at the Dallas Meeting of the Electrochemical Society, May 10, 1967, Abstract No. 83.

35. Curtis, B. J. And J. A. Wilkinson, "Preparation of Mixed Oxide Crystals by Chemical Transport Reactions, " J. Am. Ceram. Soc. 48(1), 49-50, (Jan. 1965).

36. Ferment, G. and Haskell, N. J. "Fabrication of Beryllium Oxide Radomes by Pyrolytic Deposition," AD 608486 (June 30, 1964).

37. Feuersanger, A. E., "Titanium Dioxide Dielectric Films Prepared by Vapor Reaction", Proc. IEEE 52(12), 1463-1465 (Dec. 1964).

38. Gannon, R. E., R. C. Foliveiler, T. Vasilos, "Pyrolytic Synthesis of Titanium Diboride", J. Am. Ceram. Soc. 46 (10), 496-9 (1963).

39. Gebhardt, J. J. and R. F. Cree, "Vapor Deposited Borides of Group IVA Metals", J. Am. Ceram. Soc. 48 262 AS 601861 (1965).

40. Glaister, R. M., "Solid Solution Dielectrics Based on Sodium Niobate", J. Am. Ceram. Soc. 43, 348, (July, 1960).

41. Gleason, Jr., F. R. and L. R. Watson, "Ferrite Films Prepared by Pyrohydrolytic Deposition", JAP 34, 1217, (April, 1963).

42. Haas, G., "Preparation, Properties, and Optical Applications of Thin Films of TiO_2", Vacuum, 2, 331-345, (Oct. 1952).

43. Hallander, L. E. Jr. and P. L. Castro, " Dielectric Properties of Single Crystal Nonstoichiometric Rutile, TiO_2" JAP 33, 3421-3426, (Dec. 1962).

44. Hanak, J. J., K. Strater, G. W. Cullen, "Preparation and Properties of Vapor Deposited Niobium Strannide (Nb_3Sn)", RCA Rev. 25 (3), 342-65 (1964).

45. Huber, F., "Thin Films of To Oxide for Microminiaturization, " IEEE Trans. Componett Pts. Vol. CP-11, #2 pp. 38-47 (1964)

46. IIT Research Institute, "Characterization of Ceramic Materials for Microelectronic Applications," Project G 6006-6, Rpt. #2 (June, 1966).

47. Jennings, V. J., A. Sommers, H. C. Chang, "Expitaxial Growth of SiC", J. Electrochem. Soc. 113, 728 (July, 1966).

48. Joyce, B. A. et. al. " The Epitaxial Deposition of Si on Quartz and Alumina", Trans AIME 233, 556 (1965).

49. Kalnin, I. L. and J. Rosenstock, "Vapor Deposition of Ge on Mo", J. Electrochem. Soc. 112, 329 (1965).

50. Klerer, J., "On the Mechanism of the Deposition of Silica by Pyrolytic Deposition of Silanes", J. Electrochem. Soc. 112, 329 (1965)

51. Lakshmanan, T. K., "Chemical Formation of Microcircuit Elements", AD 428590. (Dec. 1963).

52. Maxwell, K. H. and L. H. Robouin, "Chemical Vapor Deposition of Oxide Films from Volatile Chlorides I SiO_2 "Electrochem. Technol 3 (1-2) 37-40 (1965).

53. Mitchell, J. J., "Preparation and Dielectric Properties of a Multicomponent Metallic Oxide Film," AD 416330. (Mar. 1963).

54. Muller, E. K., B. J. Nicholson, G. L'E Turner, "The expiaxy of $BaTiO_3$ Films by Vapor Deposition", Brit. JAP 13, 486 (1962).

55. Muller, E. K., B. J. Nicholson, G. L'E. Turner, " The epitaxial Vapor Deposition of Perovskite Materials, " J. Electrochem. Soc. 110, 969 (Sept. 1963)

56. Peterson, D., J. Black, W. Brand, D. Dulaney, "Non Vacuum Deposition Technique for Use in Fabricating Thin Film Circuits, " AD 462743 (April 1965).

57. Peterson, D. R., Black, Brank, Tolliver (Motorola S/C Div) "Techniques For Vapor Plating Passive Film Components on Silicon Integrated Circuit Wafers," AD 475622. (Nov. 1965).

58. Rand, M. and J. L. Ashworth, " Deposition of Silica Films on Ge by the CO_2 Process," J. Electrochem. Soc. 113 48, (Jan. 1966).

59. Schaffer, P. S., "Evaluation of Vapor Deposition Growth of Oxide Single Crystals from Metal Halides," AD 616914 (May 1965).

60. Schaffer, P. S., "Vapor-Phase Growth of Single Crystals", AD 433232,

61. Schaffer, P. S., "Vapor Phase Growth of - Alumina Single Crystals", J. Am. Ceram. Soc. 48, (10), 508 (1965).

62. Seltzer, M. S., N. Alban, B. Paris, R. C. Himes, "Microscopic Measurement of Step Movement During Crystal Growth by Chemical Vapor Deposition", Rev. Sci. Inst. 36, 1423 (1965).

63. Shepherd, W. H., "Vapor Phase Deposition and Etching of Silicon", J. Electrochem, Soc. 112, 988 (1965).

64. Silvestri, V. J., "Growth Rate and Doping in the $GeCl_4$-H_2 System: Presented at the Dallas Meeting of the Electrochemical Society Meeting Abstract No. 104 May 12, 1967.

65. Steele, S., J. Poppis, R. Ellis, L. Hagen, H. Schiller, "Progress Report on Chemical Vapor Deposited Materials for Electron Tubes," AD 477126.

66. Sterling, H. F. and R. C. G. Swann, "Chemical Vapor Deposition Promoted by RF Discharge", Solid State Electron 8, 653 (1965)

67. Sterling, H. F. and R. C. G. Swann "RF Initiated Vapor Deposition of Glassy Layer," Phys. Chem. Glasses 6, 109 (1965).

68. Theurer, H. C.," Epitaxial Si Films By Hydrogen Reduction of $SiCl_4$", J. Electrochem Soc. 108 649 (July 1961).

69. Theurer, H. C. and H. Christensen, " Epitaxial Films of Si and Ge by Halide Reduction", J. Electrochem. Soc. 107, 268C (Dec. 1960).

70. Tietjen, J. J. and J. A. Amick, " The Preparation and Properties of Vapor Deposited Exitaxial GaAs by Using Arsine and Phosphine", J. Electrochem. Soc. 113, 724 (July, 1966)

71. Tung, S. K. and Caffrey, R. E., " The Deposition of Oxide on Si by Reaction of a Metal Halide with a Hydrogen/Carbon Dioxide Mixture", Trans. Met Soc. AIME 233, 572, (1965).

72. Ziegler, C.," Expitaxial In-Bs Films By Vapor Phase Transport Reaction", Solid State Electronics 6, 680-81 (Nov. - Dec. 1963)

73. Wilmsen, C. W., "Tunneling From a Metal Into a Semiconductor," Dissertation, The University of Texas, January, 1967.

74. Yeargan, J. R., "Current Mechanisms in Thin film Silicon Nitride", Dissertation to be published, the University of Texas, August, 1967.

75. Martin, H. B. "Development of Microelectronic Circuits for Linear Applications," AD 287650 (Oct. 1962).

76. Hartwig, W. H. "Metal-Insulator-Semiconductor Tunneling as a Basis for Digital Transducer Action" Bull. Amer. Phys. Soc. (Abstract), Vol 12, No. 5, Presented at Toronto Meeting, June 21-23, 1967.

77. A. Many, Y. Goldstein, and N. B. Grover, Semiconductor Surfaces, (Amsterdam: North-Holland Publishing Co., 1965).

78. J. T. Wallmark and H. Johnson, Field-Effect Transistors, Prentice Hall, Inc., Englewood Cliffs, New Jersey, 1966.

79. L. M. Terman, Solid State Electronics 5, 285 (1962).

80. K. Lehovec and A. Slobodskoy, Solid State Electronics 7, 59 (1964).

81. K. Lehovec, A. Slobodskoy, and J. Sprague, IRE Trans. on Electron Devices 8, 420 (1961).

82. S. R. Hofstein, K. H. Zaininger, and G. Warfield, Proc. IEEE 52, 971 (1964).

83. S. R. Hofstein and G. Warfield, Solid State Electronics 8 321 (1965).

84. F. D. Heiman and G. Wardield, IEEE Trans. on Electron Devices 12, 167 (1965).

85. W. A. Harrison, Phys. Rev. 123, 85 (1961).

86. R. Stratton, J. Phys. Chem Solids 23, 1177 (1962).

87. J. G. Simmons, J. Appl. Phys. 34, 1793, 2581 (1963).

88. W. Ruppel, Phys. Acta 31, 311 (1958).

89. K. H. Zaininger and G. Warfield, IEEE Trans. on Electron Devices 12, 179 (1965).

90. S. R. Pollack and C. E. Morris, J. Appl. Phys. 35, 1503 (1964).

91. Stone, J. L. and Hartwig, W. H. ," A Unique Laser Detector Utilizing the Photodielectric Effect in Colled Semiconductors", Technical Report TR-39, Laboratories for Electronics and Related Science research, The University of Texas, 161 pp. 1967.

92. Lambe, John and Klick, Clifford, "Model for Luminescence and Photoconductivity in the Sulfides', Phys. Rev. 98, 909 (1955).

93. Lambe, John "Recombination Processes in CdS" Phys. Rev. 98, 985 (1955).

Lambe, John "CdS with Silver Activator" Phys. Rev. 100 1586 (1955).

94. Kulp, B. A. " Defects in Cadmium Sulfide Crystals" J. Appl. Phys. 36, 1553 (1965).

95. Bube, R. H. PHOTOCONDUCTIVITY OF SOLIDS, New York, Wiley & Sons, 1960

96. Kronenberg, S., and Accardo, C. A., "Dielectric Changes in Inorganic Phosphors"., Phys. Rev., 101, 989, (1956).

97 Matthews, N. F. J. and Warter, P. J. "Transient Polarization in Insultating CdS" Phys. Rev. 144, 610 (1966).

98. Rose, A., CONCEPTS IN PHOTOCONDUCTIVITY AND ALLIED PROBLEMS, Interscience Publishers, New York, 1963.

VI. ATTENDANCE AT MEETINGS, PAPERS, PUBLICATIONS

A. ATTENDANCE AT MEETINGS

At the end of the first year the project director and several members of the research staff visited the Manned Spacecraft Center at Houston and presented a one-day synposium on digital transducer research which summarized the work to date.

In June, the project director presented a short paper on the metal-polymer-semiconductor thin film device at the 1967 Summer Meeting of the American Physical Siciety.

B. PAPERS AND PUBLICATIONS

Hartwig, W. H., "Metal-Insulator-Semiconductor Tunneling as a Basis for Digital Transducer Action", Bull. Amer. Phys. Soc., Ser. II, Vol. 12, No. 5, 1967.

VII. PROGRAM FOR THE SECOND YEAR

The projects which will receive major attention in the second year are: The metal-polymer-semiconductor research aimed at better understanding physical processes and development of a technique for the tunneling digital transducer; extensive research on exotic dielectric will continue in the hope of achieving an active thin film technique; continued study of the photodielectric effect with particular interest on observing the desirable effect at high temperature or longer wavelengths or both; a continuing search for new discontinous behavior in materials or combining of materials; and initiation of a project under a new faculty member, Dr. Dimiter I. Tchernev on digital information storage on magnetic thin films by Curie point writing. This work was previously done at Jet Propulsion Laboratory where Dr. Tchernev was affiliated. The results of this work have produced a significant increase (several orders of magnitude) in the density of stored digital information. It will continue at The University of Texas in the Electronic Materials Research Laboratory. In view of its direct application to digital device research, some use of the grant is deemed appropriate to get the work started.

The rapid growth of potentially useful digital device ideas has forced the entire grant to be supplemented by funds which are of a temporary nature and if continued would not be primarily responsive to the needs of NASA. We will request a substantial increase in the funding of this activity for the succeeding two-year period in a renewal request to be submitted early in the second half of the second year.